PHOSPHOREGULATION OF THE ACTIN CYTOSKELETON DURING ENDOCYTOSIS IN THE YEAST *SACCHAROMYCES CEREVISIAE*

JIN MINGJI

NATIONAL UNIVERSITY OF SINGAPORE

2007

PHOSPHOREGULATION OF THE ACTIN CYTOSKELETON DURING ENDOCYTOSIS IN THE YEAST *SACCHAROMYCES CEREVISIAE*

JIN MINGJI

A THESIS SUBMITTED FOR THE DEGREE OF DOCTOR OF PHILOSOPHY

INSTITUTE OF MOLECULAR AND CELL BIOLOGY
NATIONAL UNIVERSITY OF SINGAPORE

2007

ACKNOWLEDGEMENTS

First and foremost, I would like to express my sincere gratitude to my supervisors, **A/P Ming Jie Cai**, for his continuous guidance, encouragement and stimulating discussions that helped to sustain my interest throughout the entire course of the research project. Much appreciation is also due to the members of my post-graduate committee: **A/P Walter Hunziker**, **A/P Thomas Leung** and **Dr. Alan Munn** for their invaluable discussions and suggestions pertaining to the project.

In addition, I would also thank the past and present members in CMJ, US and WY lab for their helpful discussion, technique assistance, cooperation and friendship. Furthermore, I would like to acknowledge the contributions of the administrative and technical staffs in IMCB toward the completion of these studies.

Finally, I would like to express my deepest thanks and appreciation to my family, especially my husband, for his constant encouragement and understanding throughout these years.

Jin Mingji

Nov 2007

TABLE OF CONTENTS

List of Figures

List of Tables

ABBREVIATIONS

a.a. or aa	amino acid
Abp1p	actin-binding protein 1
ADF	actin depolymerizing factor
ADP	adenosine 5’-diphosphate
ARK	actin-regulating kinase
ATP	adenosine 5'-triphosphate
AP-1/2/3	adaptor protein-1/2/3
BAR	BIN-amphiphysin-RVS domain
bp	base pair
BSA	bovine serum albumin
°C	degree Celsius
CALM	clathrin assembly lymphoid myeloid leukaemia protein
cAMP	cyclic AMP
CC	coiled coil
CCP	clathrin-coated pit
CCV	clathrin-coated vesicle
CIP	calf intestinal phosphatase
CME	clathrin-mediated endocytosis
COOH-terminus	carboxy-terminus
DNA	deoxyribonucleic acid
DTT	dithiothreitol
ECL	enhanced chemiluminescence
E. coli	Escherichia coli
EDTA	ethylenediamine tetraacetic acid
EGTA	ethylene-bisoxyethylenenitrilo tetraacetic acid
EH	Eps15 homology
EM	electron microscopy

ENTH	Epsin amino-terminal homology
F-actin	filamentous actin
5-FOA	5-fluoro-acetic acid
FM 4-64	N-(3- triethylammoniumpropyl)-4-(p-diethylaminophenyl-hexatrienyl) pyridinium dibromide
G-actin	actin monomer
GFP	green fluorescent protein
GST	glutathione S-transferase
GTP	guanosine triphosphate
GTPase	guanosine triphosphatase
hrs	hours
HA	haemagglutinin
HIP1	Hungtingtin interacting protein-1
HRP	horseradish peroxidase
IgG	immunoglobulin G
IP	immunoprecipitation
Jas	jasplakinolide
kb	kilobase(s)
kDa	kilodalton
L	liter
LAT-A	Latrunculin-A
LB	Luria-Bertani medium
LY	Lucifer Yellow
M	molar
min	minute
ml	milliliter
mM	millimolar
μg	microgram
μm	micrometer
nm	nanometer

NH2-terminal	amino-terminal
NPF	Asp-Pro-phe motifs
N-WASP	neuronal Wiskott-Aldrich syndrome protein
OD	optical density
ORF	open reading frame
PAGE	polyacrylamide gel electrophoresis
PBS	phosphate-buffered saline
PCR	polymerase chain reaction
PEG	polyethylene glycol
PH	pleckstrin homology
PIP2	phosphatidylinositol-4,5-bisphosphate
PMSF	phenylmethylsulfonyl fluoride
PNPP	p-nitrophenylphosphate
poly-P	proline-rich region
PRD	proline- and arginine-rich domain
RFP	red fluorescent protein
RME	receptor-mediated endocytosis
rpm	revolutions per minute
sec	second
SC	synthetic complete (medium)
SDS	Sodium dodecyl sulphate
SH3	Src homology 3
SHD	Sla1 homology domain
SR	the C-terminal QxTG repeats of Sla1p
SV40	Simian virus 40
TE	Tris-EDTA buffer
TEMED	N,N,N',N'-tetramethylethylenediamine
Tris	Tris(hydroxymethyl)aminomethane
WASP	Wiskott-Aldrich syndrome protein

WT	wild type
YEPD	yeast extract-peptone-dextrose (rich medium)

SUMMARY

Endocytosis is the fundamental cellular process by which eukaryotic cells internalize materials from the extracellular environment, through invaginating plasma membrane to form endocytic vesicles. Increasing evidence underlines the importance of actin dynamics in assisting plasma membrane deformation during vesicle formation and transport. Moreover, the spatiotemporal features of actin recruitment and vesicle formation are shown to be conserved across eukaryotic evolution. In budding yeast, endocytosis occurs at the sites that coincide with the cortical actin patches, which comprise an array of proteins involved in various aspects of endocytosis and actin dynamics. Some of the molecular mechanisms by which these proteins cooperate to achieve the sequential events of endocytosis have yet remained unknown. One of the major mechanisms for regulating this process involves the phosphorylation cycles of endocytic factors by the Ark1/Prk1 kinase family. A number of endocytic components, including Pan1p, Sla1p, Scd5p, Yap1801/2p and Ent1/2p, have been identified as substrates of Prk1p, and the consensus Prk1p phosphorylation motifs have been identified as (L/I/V/M)xx(Q/N/T/S)xTG. Phosphorylation of Pan1p and other endocytic components by Prk1p leads to disassembly of the coat complex and the termination of vesicle-associated actin polymerization. Ark1p, another member of this kinase family, is also found to be essential for endocytosis and actin organization, as neither *ark1* nor *prk1* single mutant shows obvious actin and endocytic defect; while in the absence of both kinases, the defects of actin cytoskeleton and endocytosis are striking. Compared with Prk1p, Ark1p has been barely studied and its functional characteristics are essentially unknown.

This study started with demonstration of the kinase activity of Ark1p and identification of the substrates of Ark1p. The kinase activity of Ark1p appears to be comparable to that of Prk1p, and Ark1p could also phosphorylate the consensus Prk1p motifs when co-expressed in E. coli. Both Sla1p and Pan1p are identified as common substrates of Prk1p and Ark1p by in vitro kinase assay and in vivo phosphoryaltion study, while Prk1p seems to be the major kinase for Pan1p in vivo [Chapter 3]. The functional difference of the two kinases is later found to depend on their divergent non-kinase regions [Chapter 4]. Next, Arp2p, a component of Arp2/3 complex, is identified as a binding partner unique for Prk1p by testing two-hybrid interactions on cortical patch components. A short region located adjacent to the kinase domain unique to Prk1p is mapped to be required for the kinase to interact with Arp2p. Further studies demonstrated that the Prk1p-Arp2p interaction is critical for down-regulation of Pan1p [Chapter 5].

Therefore, by biochemical and genetic analysis, this study established a novel interaction between two factors in endocytosis - the actin nucleation factor Arp2/3 that promotes endocytosis and the Prk1p kinase that acts to disassemble the endocytic machinery and inhibit the actin nucleation by Pan1p. These findings reveal that, in addition to its role in the nucleation of actin polymerization, Arp2p also mediates what appears to be an auto-regulatory mechanism possibly adapted for efficient coordination of actin assembly and disassembly during endocytosis.

Chapter 1

Introduction

1.1. General introduction

All living cells are surrounded by a plasma membrane that physically separates the intracellular compartment from the extracellular environment. One of the important functions of plasma membrane is to take up and internalize extracellular materials by a dynamic process called endocytosis. During endocytosis, the extracellular materials are captured and internalized together with a portion of plasma membrane by invaginating and pinching off plasma membrane to form endocytic vesicles, which later develop into early and late endosomes and ultimately fuse with lysosome for degradation or recycle back to plasma membrane. The initial understanding of endocytosis mainly came from the morphological and biochemical studies in animal cells. Later, genetic approaches were utilized to study endocytosis in other organisms, such as *Drosophila melanogaster, Dictyostelium discoideum* and S*accharomyces cerevisiae*. The genetic studies in budding yeast *Saccharomyces cerevesiae* are especially fruitful. By isolation and characterization of endocytic mutants, a number of molecules have been identified. Their homologues are also found in mammalian endocytic pathway. Though some differences are evident between yeast and mammalian endocytosis, the underlying mechanism appears to be conserved.

During endocytic internalization steps, mechanical forces are required to work against the forces of surface tension and osmotic pressure to reshape the plasma membrane (Dai and Sheetz, 1995). Increasing evidence indicated that actin polymerization may be one of the important forces to facilitate membrane deformation and vesicle movement in both mammalian and yeast cells (Liu *et al.*,

2006; Kaksonen *et al.*, 2006). In the following sections, the relationship between actin and endocytosis will be reviewed.

1.2 Biochemical properties of Actin

Actin is a globular, 42-47 kDa protein that exists in dynamic equilibrium between two states, monomer (G actin) and filamentous polymer (F actin) (Pollard, 1990). X-ray crystallographic analysis revealed that G actin has two lobes separated by a deep cleft where the ATP molecule resides and affects the molecular conformation upon binding (Barany *et al.*, 2001). G actin can polymerize into F actin spontaneously. The actin-bound ATP will be hydrolyzed once the actin monomer incorporates into actin filaments. The actin filament has intrinsic polarity, i.e., the two ends are different. The end to which actin monomers are preferentially added is called barbed end, while the other end from which actin monomers tend to disassociate is called pointed end (Pollard and Borisy, 2003). The ATP bound actin subunits are enriched at the barbed end, while the ADP bound actin subunits are found at the pointed end. The ADP-actin subunits dissociated from pointed ends must undergo nucleotide exchange to become ATP-actin to be competent for subsequent rounds of barbed end addition. Once filament growth reaches a steady state, actin polymerization and depolymerization at the two ends are in an equilibrium. The steady-state cycling of actin subunits throughout filaments is called actin treadmilling (Nicholson-Dykstra *et al.*, 2005). Actin polymerization and treadmilling occur very slowly in vitro, but much more efficiently in vivo by assistance of a variety of actin binding proteins. Moreover, the actin filaments are further cross linked into networks

and/or anchored to specific substratum by the actin binding proteins. The biochemical features of actin, together with the actin binding proteins, allow actin filament to work as a physical force when the polymer grows beneath the plasma membrane or at one side of an object, as demonstrated in the membrane protrusion during phagocytosis and intracellular endosome movement (Figure1.1)

1.3 Actin and endocytosis in mammalian cells

1.3.1 Endocytosis in mammalian cells

Mammalian endocytosis can be classified into: clathrin-dependent pathway, the caveolar and a clathrin- and caveolae-independent pathway. Clathrin dependent endocytosis is the most extensively studied and best characterized endocytic pathway, as it is the main pathway for receptor-mediated endocytosis in most eukaryotic cells (Brodsky *et al.*, 2001). The first insight of this process came from electron microscopy studies in 1964, when the endocytic vesicles were first observed as electron-dense coated invaginations which accumulate yolk proteins at the plasma membrane in insect oocytes (Roth and Porter, 1964). By purifying coated vesicles from different cell lines, a major protein species, clathrin, was found to form the coat of all the different vesicles in different cell types (Pearse, 1976). By extensive biochemical characterization and X-ray study, the structure of clathrin coat was revealed as a triskelion in which three clathrin heavy chains tightly associated with three clathrin light chains to form a lattice (Musacchio *et al.*, 1999; Kirchhausen, 2000). Clathrin-dependent endocytosis is found to take place only at specialized sites of the cell membrane

called coated-pit zones (Santini *et al.*, 2002). However, because clathrin cannot associate directly with any known components of plasma membrane, other adapter proteins should be responsible for recruiting clathrin to the plasma membrane. The first adapter identified is AP2, a heterotetramer consisting of two large (α and β) and two small (s2 and m2) subunits, which links trans-membrane receptors destined for internalization to the clathrin lattice by association with internalization motifs within the cytoplasmic tails of these receptors (Pearse and Robinson, 1990; Schmid, 1992; Ohno *et al.*, 1995). Dynamin, a GTPase, is implicated for vesicle budding and fission (McNiven *et al.*, 2000). In addition to clathrin, AP2 and dynamin, a number of other molecules are identified to be important for clathrin dependent vesicle formation. They are proteins associated with clathrin, AP2 and dynamin and include Eps15, epsin, amphiphysin, intersectin, endophilin and rab5 (Brodsky *et al.*, 2001). Biochemical and microscopic studies have revealed some detailed processes of the clathrin mediated endocytosis (Brodsky *et al.*, 2001; Higgins and McMahon, 2002). The first step in this pathway is the reorganization and clustering of cargos by specific transmembrane receptors and other membrane adaptors. Subsequently, clathrins are recruited to the sites and oligomerized to form a clathrin coat at the plasma membrane. The coated membrane gradually undergoes deformation and invagination, and eventually forms an endocytic vesicle by membrane scission. Finally, the vesicle is uncoated and the cargo in the vesicle is delivered to early endosomes by fusing with the endosomal membrane. The cargo molecules are sorted to be either recycled back to the cell plasma membrane, or targeted for degradation in lysosomes.

1.3.2 Actin involvement in mammalian endocytosis

Actin filaments were observed to be associated with endocytic coated pits under electron microscope, providing the first clue of actin involvement in mammalian endocytosis (Salisbury *et al.*, 1980; Kohtz *et al.*, 1990). Following that, several actin dynamic perturbing pharmacological agents (such as cytochalasin D, latrunculin A and jasplakinolide) had been utilized to study the actin involvement during endocytosis in different cell types (Gottlieb *et al.*, 1993; Jackman *et al.*, 1994; Lamaze *et al.*, 1997; Fujimoto *et al.*, 2000). It was found that impaired actin dynamics had substantial but variable effect on endocytosis in different cell types. Now it is clear that actin polymerization is essential for the formation of membrane protrusions in macropinocytosis and phagocytosis (May and Machesky, 2001; Welch and Mullins, 2002), and the internalization process in caveolae-mediated endocytosis (Pelkmans *et al.*, 2002)(Figure 1.1).

Though there are debates on the role of actin in clathrin dependent endocytosis, evidence is accumulating in recent years supporting the involvement of actin polymerization in clathrin dependent endocytosis as depicted in Figure 1.1. With actin depolymerization drugs, actin polymerization was found to be necessary for clathrin-mediated endocytosis (Merrifield *et al.*, 2002; Yarar *et al.*, 2005; Boucrot *et al.*, 2006). On the other hand, actin filaments were also found to colocalize with clathrin-mediated endocytic sites (Shupliakov *et al.*, 2002). In addition, a large number of protein–protein interactions have been discovered to link the endocytic machinery to the actin cytoskeleton(Qualmann and Kessels, 2002; Engqvist-Goldstein and Drubin, 2003). Moreover, using green fluorescent

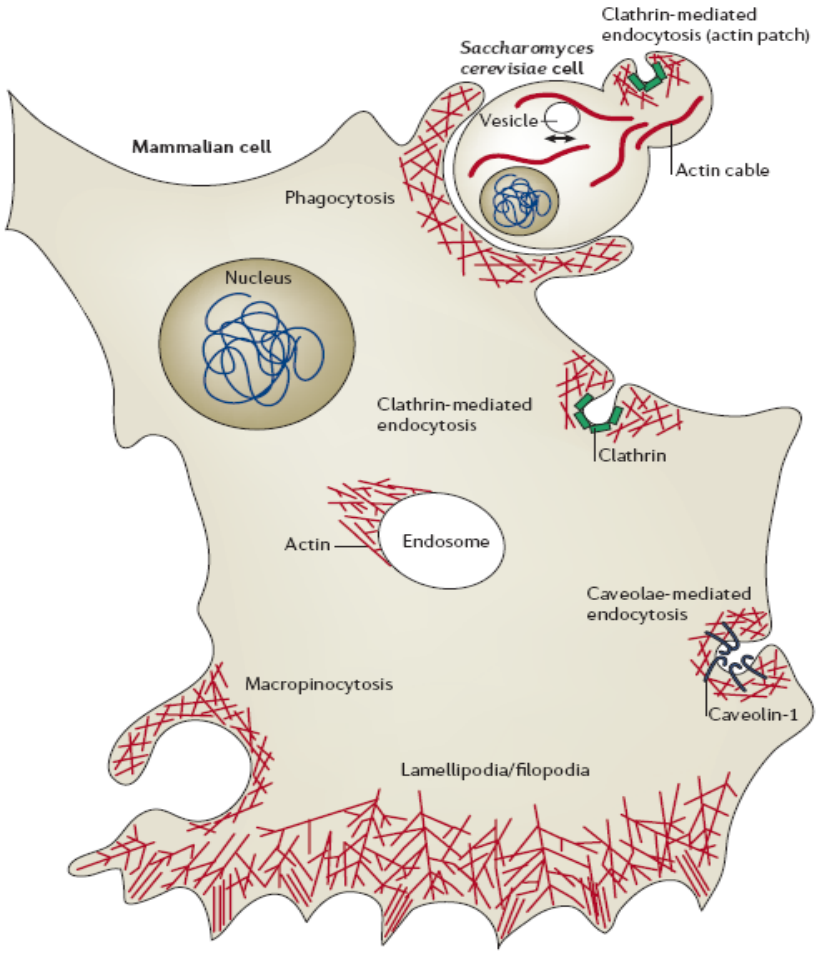

Figure 1.1 Actin-polymerization-motivated processes in mammalian and budding yeast cells.

The dynamic polymerization of actin filaments (red) is involved in different processes that reshape or move cellular membranes. These processes include different forms of endocytic pathways at the plasma membrane — that is, clathrin-mediated endocytosis in *Saccharomyces cerevisiae* and mammalian cells, as well as caveolae-mediated endocytosis, macropinocytosis and phagocytosis in mammalian cells. In addition, actin assembly plays a role in the movement of endosomes and/or endocytic vesicles. In mammalian cells, endosomes move by actin 'rocketing', whereas in *S. cerevisiae*, endocytic vesicles move together with actin cables as they are being assembled by formin proteins. Finally, the protrusion of lamellipodia and filopodia in migrating mammalian cells is dependent on actin polymerization. [Figure adapted by permission from Macmillan Publishers Ltd: [Nature Reviews Molecular Cell Biology] (Kaksonen et al., 2006), copyright (2006)]

protein (GFP) tagged or fluorescently labeled actin, total internal reflection fluorescence (TIRF) microscopy revealed that actin filaments as well as the endocytic components were assembled and disassembled at endocytic sites in a highly ordered manner. The actin filaments appear when the coated endocytic membrane starts to invaginate to form the clathrin coated vesicles, and disappear coincidently with the scission of the endocytic vesicles (Merrifield *et al.*, 2002; Merrifield, 2004; Yarar *et al.*, 2005), indicating actin polymerization may have roles in the vesicle invagination and pinching off. Consistently, the scission of clathrin coated vesicles was dramatically reduced when the cells were treated with actin polymerization inhibitors (Merrifield *et al.*, 2005).

1.4 Actin and endocytosis in yeast

1.4.1 Actin structures in yeast

Budding yeast cells contain three distinct actin structures that are visible by fluorescence microscopy of Rhodamine-phalloidin stained cells: cortical actin patches, actin cables and a contractile actin ring (Adams and Pringle, 1984; Kilmartin and Adams, 1984; Amberg, 1998); Figure1.2). Actin patches are spots distributed over the cell surface. Actin cables are fibers coursing through the cells in parallel with the long axes of the cells. The nucleation of actin cables is activated by yeast formins (Bni1 and Bnr1), and crucial for polarized movement of traffic vesicles for growth. Actin contractile rings are actin bands formed transiently at bud necks of large budded cells, and important for cytokinesis (Sanders and Field, 1994; Bi *et al.*, 1998; Lippincott and Li, 1998).

These actin structures are highly dynamic, undergoing extensive rearrangements in accordance with polarity switches during the cell cycle. In G1 cells before START (the point of commitment to a new cell cycle), actin cables and patches are distributed randomly resulting in isotropic cell expansion. Once the G1 cell reaches a critical size, the budding site is formed. Actin cables are oriented toward this incipient bud site and patches converge to this region, which initiates a transition from isotropic to apical cell growth mode. Once the orientation of cables is established, secretory vesicles containing building materials for new cell wall and plasma membrane are transported along the cables and deposit the contents at the growth region. As a bud emerges, cables extend from the mother cell into the bud, and patches remain concentrated at the bud tip, leading to a period of bud elongation. Later, near the end of G2 phase, the actin cables and patches in the bud become randomly distributed, causing a switch from apical to isotropic bud growth. At this stage, the cables in the mother cell still extend into the bud, ensuring that only the bud grows. At the end of bud growth, actin cables and patches redistribute randomly in both the mother cell and bud (Adams and Pringle, 1984; Kilmartin and Adams, 1984; Novick and Botstein, 1985; Lew and Reed, 1993; Welch *et al.*, 1994; Lew and Reed, 1995; Kron and Gow, 1995). This is quickly followed by the congregation of actin to the sides of the neck to form contractile actin rings, which is a prerequisite for cytokinesis (Lew and Reed, 1993; Lew and Reed, 1995).

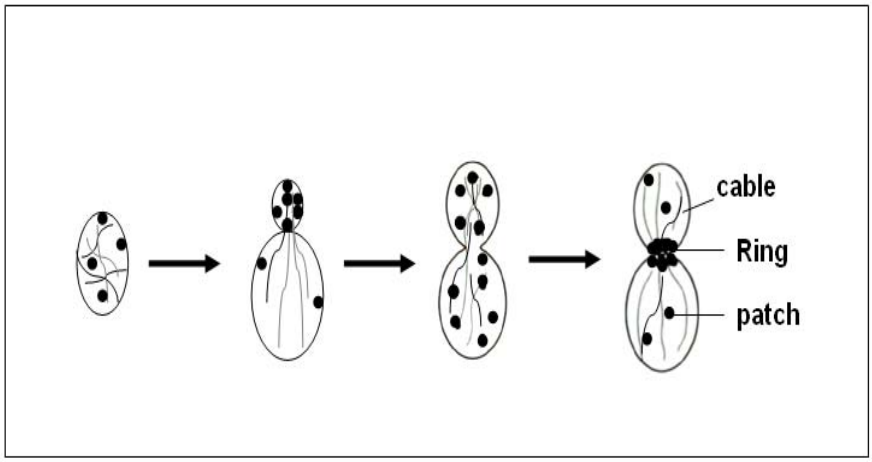

Figure 1.2 Organization of the actin cytoskeleton in *S. cerevisiae*

Actively growing yeast cells contain three visible F-actin structures: cortical actin patches, polarized actin cables, and a cytokinetic actin ring, which are undergoing extensive rearrangements in accordance with polarity switches during the cell cycle.

1.4.2 Endocytosis in *Saccharomyces cerevisiae*

The budding yeast *Saccharomyces cerevisiae* is an excellent model for endocytosis study due to its advantages in genetic manipulation. Non-essential genes can easily be disrupted from the yeast genome to directly address their functions in a given cellular process. The function of essential genes can also be tested by creating temperature sensitive (ts) or other conditional alleles, which are only inactivated at a given temperature or under certain conditions. In addition, various genetic screen strategies can be set up to isolate the mutants defective in specific cellular processes in yeast.

In order to screen for yeast mutants defective in endocytosis, it is critical to set up assays that can measure the cellular uptake defects. Various assays were

developed in yeast to assess the internalization of distinct endocytic pathways. Receptor mediated endocytosis can be followed by quantitative evaluation of the uptake of radioactively labeled α factor (Dulic *et al.*, 1991). To assess fluid phase endocytosis in yeast, two fluorescent dyes are commonly used: lucifer yellow (LY), and FM 4-64 (Riezman, 1985; Dulic *et al.*, 1991; Vida and Emr, 1995). By using different assays and screening procedures, a number of endocytosis mutants (such as *end*, *ren, dim* mutants) were isolated (Chvatchko *et al.*, 1986; Davis *et al.*, 1993; Raths *et al.*, 1993; Munn and Riezman, 1994; Wendland *et al.*, 1996; Luo and Chang, 1997; D'Hondt *et al.*, 2000; Munn, 2001), and many important endocytic components were identified. So far, over fifty genes that are important for receptor internalization have been isolated, and most of the proteins encoded by these genes have homologues in mammalian cells or have domains that share homology with that present in mammalian endocytic proteins (Engqvist-Goldstein and Drubin, 2003) (Figure1.3).

Latest development in live-cell imaging microscopy, coupled with genetic, biochemical and pharmacological tests of function, greatly improved our understanding of the receptor-mediated endocytosis in budding yeast. Total internal reflection fluorescence (TIRF) and multicolor real-time fluorescence microscopy, in particular, together with particle tracking algorithms permit tracking the behavior of a particular endocytic molecule during endocytosis. Similar to the observations in the mammalian cells, the yeast endocytic components are found to be assembled and disassociated at endocytic sites in a highly ordered sequence (Merrifield, 2004; Kaksonen *et al.*, 2006).

Saccharomyces cerevisiae proteins	Mammalian proteins	Functions
Abp1	ABP1	Arp2/3-complex activator in *S. cerevisiae*, actin-binding protein, scaffold protein
Act1	Actin	Cytoskeletal filaments
Ark1, Prk1	AAK1, GAK	Protein phosphorylation
Bbc1	–	WASP regulator
Bzz1	Syndapin	WASP-interacting protein
Capping proteins (Cap1/2)	Capping proteins (CAPZ-α, CAPZ-β)	Barbed-end actin-filament capping proteins
Chc1, Clc1	Clathrin	Vesicle coat component
Inp52	Synaptojanin	PtdIns(4,5)P_2 5-phosphatase
Las17	WASP, N-WASP	Arp2/3-complex activator
Myo3, Myo5	Type-I myosins	Arp2/3-complex activator in *S. cerevisiae*, motor protein
Pan1 complex (Pan1, Sla1, End3)	Intersectin, EPS15	Adaptor protein, Arp2/3-complex activator (Pan1 in *S. cerevisiae*), WASP regulator (Sla1, Intersectin)
Rvs161, Rvs167	Amphiphysin	Membrane bending or curvature sensing
Sac6	Fimbrin	Actin-filament-crosslinking protein
Sla2	HIP1R	Actin-binding protein, PtdIns(4,5)P_2-binding protein
Vrp1	WIP	WASP-interacting protein
–	Cortactin	Arp2/3-complex activator
–	Dynamin-1,-2	GTPase, vesicle scission

Figure 1.3 *Saccharomyces cerevisiae* and mammalian protein homologies.

This table gives descriptions of the key endocytic proteins in *S. cerevisiae*, together with mammalian homologies and their functions. The '–' symbol indicates that there is no known homologue. AAK1, adaptor-protein-complex-2-associated kinase-1; Abp1/ABP1, actin-binding protein-1; Ark1, actin-regulating kinase-1; Arp2/3, actin-related protein-2/3; Cap 1/2, barbed-end capping proteins; CAPZ, capping protein muscle Z-line; Chc1, clathrin heavy chain-1; Clc1, clathrin light chain-1; EPS15, epidermal-growth-factor-receptor-pathway substrate-15; GAK, cyclin-G-associated kinase; HIP1R, Huntingtin-interacting protein-1 related; Myo, myosin; PtdIns(4,5)P2, phosphatidylinositol-4,5-bisphosphate; Rvs, reduced viabililty upon starvation; (N-)WASP, (neuronal) Wiskott–Aldrich syndrome protein; WIP, WASP-interacting protein. [Figure adapted by permission from Macmillan Publishers Ltd: [Nature Reviews Molecular Cell Biology] (Kaksonen et al., 2006), copyright (2006)]

Depending on the cargos and the respective assay methods, endocytosis in budding yeast has been classified into two main pathways: receptor-mediated endocytosis and fluid-phase endocytosis. Recepter-mediated endocytosis can be further divided into ubiquitin–dependent and NPFX(1,2)D-dependent internalisation based on the target signals (Tan *et al.*, 1996; Hicke, 2001; Howard *et al.*, 2002).

However, it should be noted that though there are many similarities between yeast and mammalian endocytosis, there are also some differences between them. In yeast, clathrin, AP2 and dynamin are not as critical for endocytosis as their homologues in mammalian cells, while actin polymerization is strictly required in budding yeast endocytosis (Geli and Riezman, 1998).

1.4.3 Actin involvement in yeast endocytosis

The actin polymerization and turnover are essential for yeast endocytic internalization, because treatment of yeast cells with latrunculin-A (an actin monomer sequester leading to rapid disassembly of F-actin), or jasplakinolide (an actin filament stabilizer) blocked endocytic internalization (Ayscough *et al.*, 1997; Ayscough, 2000). Approximately one third of the known endocytic proteins directly regulate actin assembly and/or bind to actin (Raths *et al.*, 1993; Munn *et al.*, 1995). In addition, the majority of endocytic mutants identified hitherto have defects in the actin cytoskeleton organization. Also, the severity of the endocytic defect is generally correlated with the severity of the actin phenotype.

Recently dual color real-time fluorescence microscopy has been used to investigate the spatiotemporal correlation of actin assembly and endocytic

proteins during endocytic internalization (Kaksonen *et al.*, 2003; Kaksonen *et al.*, 2005). The transient actin burst was found to strictly appear at preformed endocytic coated structures at the yeast endocytic site, while actin disassembly was found to occur immediately after vesicle scission (Merrifield *et al.*, 2005). Such dynamic characteristics of actin indicate that actin polymerization could play roles in yeast endocytosis invagination, constriction and scission. Consistently, when actin polymerization is blocked by latrunculin A, the clathrin coats and coat-associated proteins are stabilized at the plasma membrane and the internalization movement is completely blocked (Kaksonen *et al.*, 2003; Kaksonen *et al.*, 2005; Newpher *et al.*, 2005).

1.4.4 A dynamic picture of yeast actin and endocytosis

Based on their dynamic features during endocytosis, the endocytic components are proposed to function as four groups of dynamic modules: the coat, the Wiskott–Aldrich syndrome protein (WASP)–myosin complex, the actin network and the amphiphysin complex (Kaksonen *et al.*, 2005) (Figures 1.4). First, the coat module comes to the specified endocytic sites and thereby initiates the endocytic coat assembly. This module contains clathrin, Ede1p, Sla1p, Pan1p, End3p, and Sla2p, and may also include Ent1/2p and Yap1801/2p (Newpher *et al.*, 2005). These coat proteins may help to recognize and cluster endocytic targets which are modified by ubiquitin or contain a unique signal motif. After assembly on the plasma membrane, these proteins remain stationary for about one minute, and then move inward with the forming vesicle. The second group, the WASP/Myo module proteins, which contain at least two Arp2/3 complex

activators, such as Las17p (yeast WASP homolog) and the type I myosin Myo5p, are recruited to surround the coated endocytic site. As the Arp2/3 complex activators, the WASP/Myo module proteins are believed to initiate the actin filaments network formation at the endocytic sites in response to some signals, and thus generate force to drive membrane deformation and inward movement. A few seconds after the arrival of the WASP/Myo module, the actin module proteins start to be assembled at the endocytic site. Actin and some actin associated proteins, such as Cap1/2p, Sac6p, Abp1p, and the Arp2/3 complex, belong to this module. All the proteins in this module depend on actin polymerization for their cortical localizations, as Latrunculin A treatment will prevent their patch localization. The lastly joined module is the amphiphysin module. It is composed of Rvs161p and Rvs167p. The BAR domains of Rvs161p and Rvs167p are shown to promote membrane curvature *in vitro* (Peter *et al.*, 2004). They appear soon after actin polymerization begins and remain for a short while, then move rapidly inward, and disassociate from endocytic coat. The rapid inward movement was speculated to coincide with the vesicle scission from the plasma membrane (Kaksonen *et al.*, 2005).

1.4.5 Actin assembly and force generation

The next question would be how the actin polymerization is incorporated into endocytic machinery during internalization process. A detailed understanding of actin patch ultra-structure would provide important information. Recently, rapid-freeze deep-etch electron microscopy revealed ultra-structure of actin patches: actin filaments form branched, cone shaped network at the cell

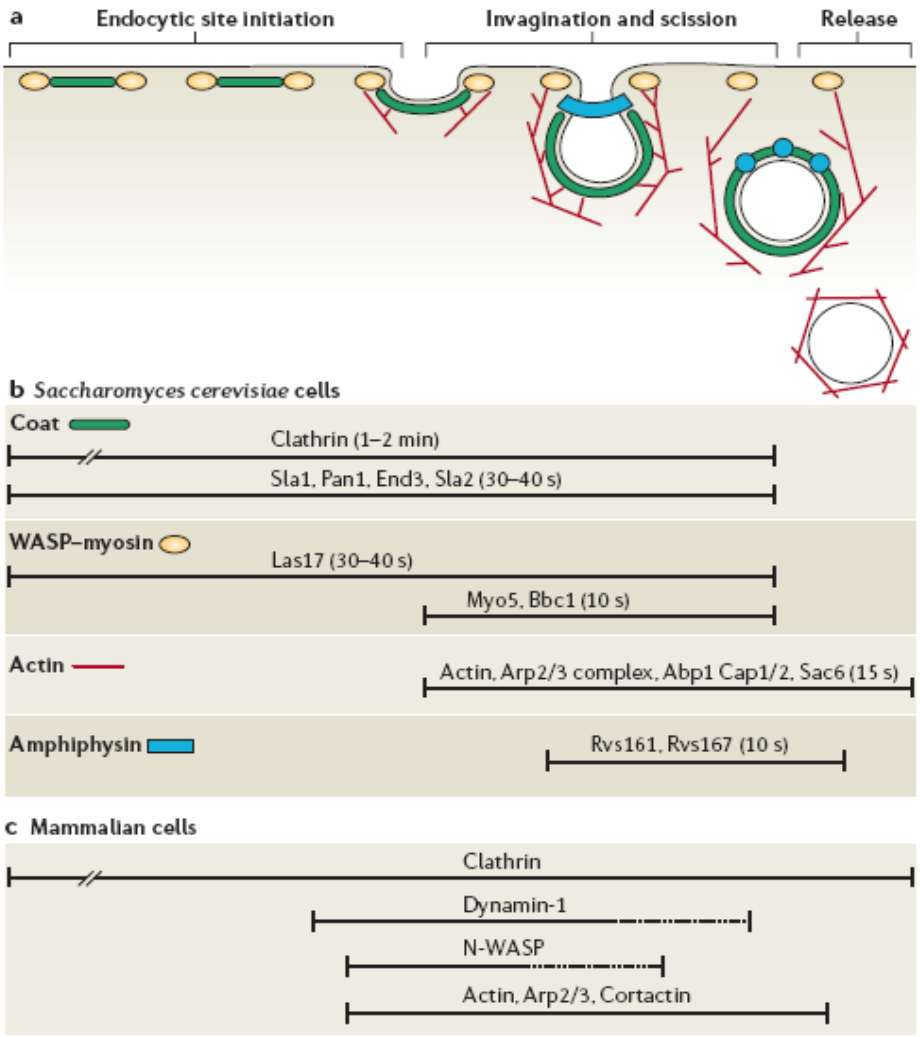

Figure 1.4 The sequential assembly of actin filaments and endocytic components at endocytic sites.
a. The different steps of endocytic internalization: endocytic site initiation, membrane invagination and scission, and vesicle release. The four protein modules that are involved in endocytic internalization in *Saccharomyces cerevisiae* are shown schematically — that is, the coat (green), the Wiskott–Aldrich syndrome protein (WASP)–myosin complex (yellow), the actin network (red) and the amphiphysin complex (blue). Components of these different protein modules are assembled and disassembled dynamically.
b. The temporal localization of the constituent proteins for each module in *S. cerevisiae*. **c.** The approximate temporal localization of proteins during endocytic internalization in mammalian cells. Dashed lines indicate ambiguity in the time frame of the protein dynamics. [Figure adapted by permission from Macmillan Publishers Ltd: [Nature Reviews Molecular Cell Biology] (Kaksonen et al., 2006), copyright (2006)]

cortex, with Arp2/3 complex restricted to the apexes of the mound (Mulholland *et al.*, 1994; Young *et al.*, 2004; Rodal *et al.*, 2005). The position of Arp2/3 complex suggests that the majority of the actin filament barbed end oriented to the cell cortex. This assignment of actin filament polarity at the actin patches is also supported by photo-bleaching the actin filaments in the live *sla2*Δ and *sla1*Δ *bbc1*Δ mutant cells (Kaksonen *et al.*, 2003; Kaksonen *et al.*, 2005).

Based on all the previous data and recent live-cell image and electron microscopy findings, a schematic working model for actin polymerization in the yeast endocytic machinery was proposed (Kaksonen *et al.*, 2006; Figure1.4). When the endocytic coat proteins are assembled at the endocytic sites, the Arp2/3 activators (including Las17p and Myo5p) are recruited to the rim of the invaginating endocytic coat. They not only associate with endocytic coat, but also efficiently activate the Arp2/3 complex to nucleate actin filaments. The actin filaments are further crosslinked by fimbrin/Sac6p. Some endocytic proteins (such as Sla2p and Pan1p) which associate with coat can also bind with actin filaments. Therefore, these actin filaments are fixed to the endocytic coat by these linkers and the continual actin filament growth at the opposite ends generate force to push the plasma membrane and results in the inward movement of the coat membrane (Mulholland *et al.*, 1994; Rodal *et al.*, 2005; Kaksonen *et al.*, 2006).

1.4.6 Control of actin polymerization during endocytosis

As the actin polymerization is very slow in vitro, a number of actin binding

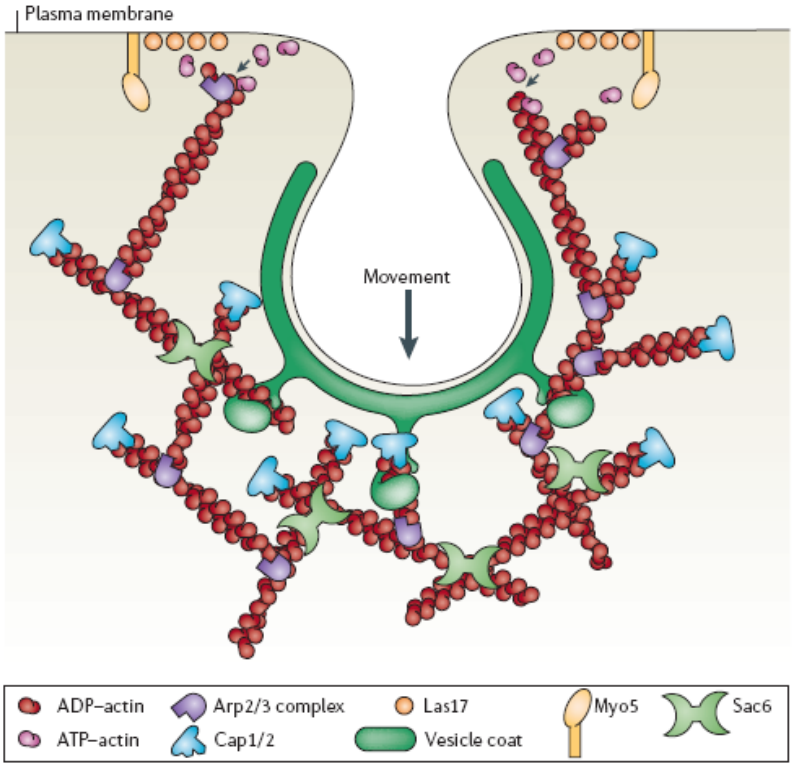

Figure 1.5 Working model of actin polymerization in the yeast endocytic machinery

This schematic diagram illustrates putative functions of different actin-cytoskeleton proteins during endocytic internalization in *Saccharomyces cerevisiae*. Las17 (yeast Wiskott–Aldrich syndrome protein) together with the myosins Myo3 (not shown) and Myo5 activate the actin-related protein-2/3 (Arp2/3) complex at the cell surface. Myosins might also generate force on the actin network or anchor the actin filaments to the plasma membrane through their motor domains. The activated Arp2/3 complexes form branched actin filaments that grow through the addition of ATP–actin monomers near the plasma membrane. Older filaments are capped at their barbed ends by capping proteins (Cap1/2). The branched filaments are further crosslinked by Sac6. The crosslinked actin network is linked to the underlying vesicle coat by actin-binding proteins such as Sla2 and Pan1, which are represented by green hand-like structures. The growth of the actin network leads to the invagination of the coated membrane. [Figure adapted by permission from Macmillan Publishers Ltd: [Nature Reviews Molecular Cell Biology] (Kaksonen et al., 2006), copyright (2006)]

proteins are involved in the regulation of actin polymerization in the cells to adapt to the requirement of a particular cellular process. The actin polymerization at the endocytic site is initiated by Arp2/3 complex, which nucleate actin assembly by mimicking actin filament barbed end (Welch and Mullins, 2002). In *S. cerevisiae,* there are five potential Arp2/3-complex activators at endocytic sites — Las17p (yeast WASP), Pan1p (yeast Eps15), Myo3p, Myo5p (motor proteins) and Abp1p (actin binding protein-1) (Kaksonen *et al.*, 2003; Engqvist-Goldstein and Drubin, 2003; Jonsdottir and Li, 2004; Sirotkin *et al.*, 2005). The live-cell image studies of four of these proteins (Las17p, Pan1p, Myo5p and Abp1p) show that each of them behaves in a temporally and spatially distinct manner, which indicates that they might control the actin polymerization at different stages during vesicle formation and inward movement. Consistently, mutations blocking the Arp2/3 activity of Las17p, Pan1p, or Myo5p lead to severe defects in actin organization and endocytosis (Sun *et al.*, 2006).

To coordinate the actin assembly and vesicle membrane formation, the activities of these Arp2/3 complex activators must be under controls as well. For example, Las17p assembles about 1 minute earlier before the emergence of actin filaments at the endocytic site, indicating Las17p activates Arp2/3 complex to nucleate actin not immediately after its assembly, but likely to be in response to some signals. The signals to activate these Arp2/3 complex activators during specific endocytic steps are unknown yet. But, in vitro biochemical analysis show that two coat module proteins, Sla1p and Bbc1p, are able to inhibit Las17p, whereas the SH3 domain of Bzz1p (a yeast syndapin-like protein) relieves Las17p inhibition (Rodal *et al.*, 2003; Sun *et al.*, 2006). On the other hand, Sla2

(yeast Hip1R) is also found to inhibit Pan1p to activate Arp2/3 complex in vitro (Toshima *et al.*, 2006).

1.4.7 Phospho-regulation of actin polymerization and endocytosis in budding yeast by Ark1/Prk1 kinase

Endocytosis, like some other important biological processes, is regulated by phosphorylation. Reversible phosphorylation of endocytic proteins appears to be important for the dynamic assembly and disassembly of endocytic coat. One of the best characterized mechanisms is phosphoregulation by Ark1/Prk1 kinase family which is conserved from yeast to mammalian cells (Smythe and Ayscough, 2003). The members of this kinase family include mammalian cyclin-G-associated kinase (GAK) and adapter-associated kinase (AAK1), as well as yeast Ark1p, Prk1p and Akl1p, featured by their homology in an N-terminal kinase domain (Figure1.6).

GAK1 and AAK1 were identified as components of endocytic coat complex, and found to phosphorylate AP-1/AP-2 μ chains (Wilde and Brodsky, 1996; Umeda *et al.*, 2000; Olusanya *et al.*, 2001; Conner and Schmid, 2002).

The first kinase of this family, Prk1p, was identified in two independent studies. In one study, Prk1p was isolated in a genetic screen for extragenic suppressors of *pan1-4*, a temperature sensitive Pan1 mutant defective in actin cytoskeleton organization (Zeng and Cai, 1999). In this study, the kinase-substrate relationship between Prk1p and Pan1p was also established.

Moreover, the typical Prk1p phosphorylation motif (LxxQxTG), which is

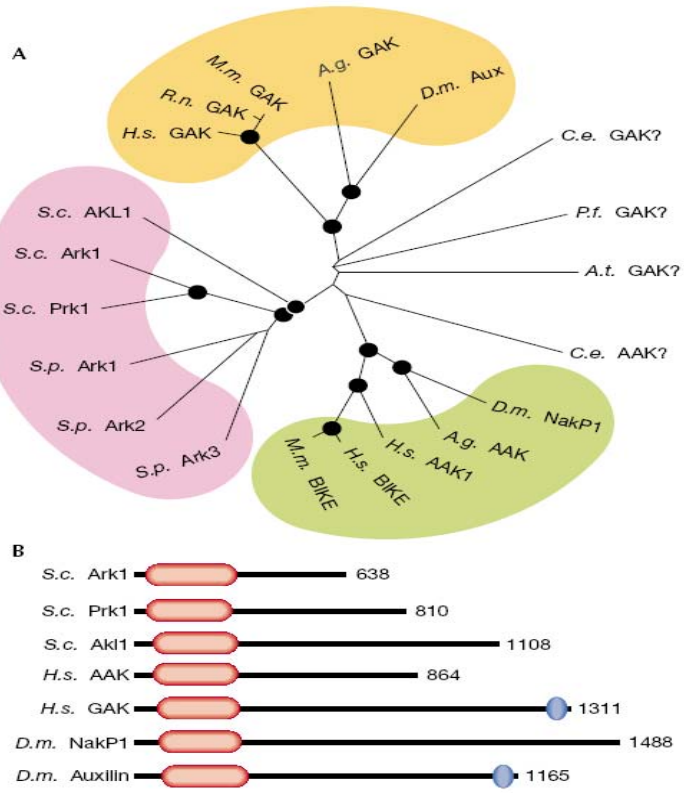

Figure 1.6 Ark/Prk kinase family members.

A. Unrooted phylogenetic tree of the kinase domains of the Ark1/Prk1 family produced from alignments generated using ClustalX software. The black circles indicate nodes that scored a significance of greater than 90% probability. Coloured areas denote a possible subfamily. The yeast kinase members all fall into a distinct group (pink) as do the AAK1-related (green) and GAK-related (yellow) members.

B. Diagram of Ark1/Prk1 kinase domain structures. In all cases, the kinase domain is near the amino terminus (red lozenge). The length of the region downstream of the kinase domain is extremely variable. In the kinase domains, Ark1 is 73% identical to Prk1, 48% to Akl1, and 38% to both NakP1 and AAK1. The kinase domain of AAK1 is 66% identical to NakP1 and 39% to GAK. AAK, adaptor-associated kinase; BIKE, BMP2-inducible kinase; GAK, cyclin-G-associated kinase; NakP1, Numb-associated kinase P1; Aux, Auxilin; *A.g.*, *Anopheles gambiae*; *A.t.*, *Arabidopsis thaliana*; *C.e.*, *Caenorhabditis elegans*; *D.m.*, *Drosophila melanogaster*; *H.s.*, *Homo sapiens*; *M.m.*, *Mus musculus*; *P.f.*, *Plasmodium falciparum*; *R.n.*, *Rattus norvegicus*; *S.c.*, *Saccharomyces cerevisiae*; *S.p.*, *Schizosaccharomyces pombe*. [Figure reproduced with permission from (Smythe and Ayscough, 2003) the Nature Publishing Group]

highly repeated in Pan1 N-terminal region, was identified. In another study, Ark1p was first isolated in a yeast two-hybrid screen to identify Sla2p binding partners. Prk1p, which has a similar kinase domain to Ark1p, was also characterized (Cope *et al.*, 1999). In the following years, several coat proteins, Sla1p, Ent1/2p, YAP1801/2p and Scd5p, which contains clustered multiple sites similar to Prk1p phosphorylation motif, were also identified as Prk1p substrates (Zeng *et al.*, 2001; Watson *et al.*, 2001; Huang *et al.*, 2003; Henry *et al.*, 2003). In all of the Prk1p substrates, these phosphorylation sites are distributed in the regions required for interaction with other endocytic proteins, suggesting that phosphorylation may regulate the assembly of endocytic complexes. This idea is supported by the failure of binding between phosphor-Pan1p and Sla1p in *in vitro* binding assay. Moreover, over-expression of Prk1p results in the dissociation of Sla1p from Pan1p-containing complexes in gel- filtration experiment, which also supports that the consequences of phosphorylation is to the disassociate the coat protein complex (Zeng *et al.*, 2001).

Prk1p and Ark1p are functionally redundant. Deletion of Prk1p or Ark1p alone does not have any apparent defects in actin patch and endocytosis regulation, while simultaneous disruption of both genes resulted in severe defects in actin organization, featured by large actin clumps (Cope *et al.*, 1999). However, loss of Prk1p, but not Ark1p, is synthetic lethal with *sla2*Δ, and forms actin clumps in an *abp1*Δ mutant, indicating that they have distinct functions. But until now, Ark1p function has been rarely studied.

Another important feature of Prk1p and Ark1p is their C-terminal poly proline motif. This motif, which interacts with the Src-homology 3 (SH3) domain of the actin-binding protein Abp1p, is required for proper actin patch localization for both kinases (Fazi *et al.*, 2002). However, *abp1*Δ mutant does not show any actin defect similar to *ark1*Δ *prk1*Δ mutant, which may be explained by the residual patch localization of Prk1p in *abp1*Δ mutant. It is also possible that Ark1p and Prk1p may have important function outside of the actin patch.

In this study, we set out to study the distinct functions of Ark1p and Prk1p during actin assembly in yeast endocytosis by genetic, biochemistry and cell biology methods.

CHAPTER 2

Materials and Methods

2.1 Reagents

All laboratory chemicals were purchased from Sigma-Aldrich Co. (St.Louis MI, USA) or BDH Ltd. Media components were from Difco Laboratories (USA) and Sigma Chemical Company (USA). Enzymes were from New England Biolabs (Boston, MA, USA) and Roche Diagnositics (Mannheim, Germany). Radioisotope was purchased from New England Nuclear Inc. Oligonucleotides used in this study were synthesized by Research Biolabs (Singapore) or Sigma-Aldrich-Proligo (Singapore).

For immunoprecipitation of Pan1p-Myc or Myc-Sla1p, Goat-anti Myc conjugated beads (New England Biolabs) were utilized. Rabbit-anti HA conjugated beads (New England Biolabs) were used to immunoprecipitate HA-Prk1p, HA-Ark1p or HA-Ark1^{D159Y} to do the in vitro kinase assay. The following antibodies were used for immuno-detection: mouse monoclonal α-Myc (Santa Cruz Biotechnology) at 1:500 for detection of Pan1p-Myc and Myc-Sla1p; rabbit polyclonal α-phosphor-threonine at 1:250 (Zymed, Invitrogen) for detection of phosphor-threonine modification of Pan1-Myc and Myc-Sla1p immunoprecipitated from different kinase mutant backgrounds; and rabbit polyclonal α-phosphothreonine at 1:5000 (Zymed, Invitrogen) for detection of phosphothreonine modification of purified GST fusion substrates from *E.coli* co-expression kinase assay. HRP-conjugated sheep anti-mouse IgG (Amersham) was used as secondary antibody.

2.2 Strains and culture conditions

The *E. coli* strain DH5α (GIBCO BRL, USA) was used as the host strain in this study for DNA recombination and plasmid amplification. The *E. coli* strain BL21 Gold (Stratagene) was used as the host strain for GST or His fusion protein expression. The *E. coli* cells were cultured at 37^{o}C in LB broth (1% bacto-tryptone, 0.5% bacto-yeast extract, 1% NaCl, pH 7.0) or on LB agar plates (LB containing 2% bacto-agar) with 100 μg/ml Ampicilin (Sigma) or 25 μg/ml Kanamycin (Sigma) added to the media to select for *E. coli* cells carrying recombinant plasmids.

Yeast cells were grown in standard yeast extract-peptone-dextrose (YEPD; 1.1% yeast extract, 2.2% peptone, 0.006% adenine and 2% glucose) or synthetic complete medium (SC; 0.67% yeast nitrogen base without amino acids, 2% D-glucose and 0.2% amino-acids mix). For the selection and maintenance of some nutritional markers that were introduced into yeast strains, appropriate selective media (SC without appropriate amino acid) were used. Wild-type cells were grown at 30°C with good aeration while temperature-sensitive mutants were cultured at the permissive temperature of 25°C and analyzed at the restrictive temperature of 37°C. To induce the expression of genes under the *GAL1* promoter, cells were grown overnight in the medium with 2% raffinose instead of D-glucose as the carbon source, and induced 1 to 4 hours with 2% Galactose added to the culture. The yeast strains used in this study are listed in the Table 1.

Table 1.Yeast Strains Used in This Study

Strain	Genotype and sorce
W303-1A	*MAT***a** *ade2-1 trp1-1 can1-100 leu2-3,112 his3-11,15 ura3-1* (Laboratory collection)
SFY526	*MAT***a** *ura3-52 his3-200 ade2-101 lys2-801 trp1-901 leu2-3,112 canr gal4-542 gal80-538 URA3:: GAL1-lacZ* (CLONTECH, USA)
YMC410	*MAT* **a** *ade2-1 trp1-1 can1-100 leu2-3,112 his3-11,15 ura3-1 prk1Δ::HIS3* (Laboratory collection)
YMC411	*MAT* **a** *ade2-1 trp1-1 can1-100 leu2-3,112 his3-11,15 ura3-1 prk1Δ::HIS3 akl1Δ::URA3* (Laboratory collection)
YMC412	*MAT* **a** *ade2-1 trp1-1 can1-100 leu2-3,112 his3-11,15 ura3-1 prk1Δ::HIS3 akl1Δ::URA3 ark1Δ:: LEU2* (Laboratory collection)
YMC413	*MAT***a** *ade2 trp1 can1 leu2 his3 ura3 pan1-4 prk1Δ:: HIS3* (Laboratory collection)
YMC414	*MAT* **a** *ade2-1 trp1-1 can1-100 leu2-3,112 his3-11,15 ura3-1 prk1Δ::HIS3 ark1Δ:: LEU2* (Laboratory collection)
YMC511	*MAT* **a** *ade2-1 trp1-1 can1-100 leu2-3,112 his3-11,15 ura3-1 pan1::PAN1-Myc-TRP1* (This study)
YMC512	*MAT* **a** *ade2-1 trp1-1 can1-100 leu2-3,112 his3-11,15 ura3-1 prk1Δ::HIS3 pan1:: PAN1-Myc-TRP1* (This study)
YMC503	*MAT* **a** *ade2-1 trp1-1 can1-100 leu2-3,112 his3-11,15 ura3-1 prk1Δ::HIS3 akl1Δ::URA3 pan1:: PAN1-Myc-TRP1* (This study)
YMC504	*MAT* **a** *ade2-1 trp1-1 can1-100 leu2-3,112 his3-11,15 ura3-1 prk1Δ::HIS3 akl1Δ::URA3 ark1Δ:: LEU2 pRS314-PAN1-Myc-TRP1* (This study)
YMC505	*MAT* **a** *ade2-1 trp1-1 can1-100 leu2-3,112 his3-11,15 ura3-1 sla1:: Myc-SLA1-TRP1* (This study)

YMC507	*MAT* **a** *ade2-1 trp1-1 can1-100 leu2-3,112 his3-11,15 ura3-1 prk1Δ::HIS3 akl1Δ::URA3 sla1:: Myc-SLA1-TRP1* (This study)
YMC508	*MAT* **a** *ade2-1 trp1-1 can1-100 leu2-3,112 his3-11,15 ura3-1 prk1Δ::HIS3 akl1Δ::URA3 ark1Δ::LEU2 pRS314 –Myc-SLA1-TRP1* (This study)
YMC509	*MAT* **a** *ade2-1 trp1-1 can1-100 leu2-3,112 his3-11,15 ura3-1 prk1Δ::HIS3 ark1Δ::LEU2 pan1:: PAN1-Myc-TRP1* (This study)
YMC510	*MAT* **a** *ade2-1 trp1-1 can1-100 leu2-3,112 his3-11,15 ura3-1 arp2::Arp2-HA-LEU2* (This study)
YMC513	*MAT* **a** *ade2-1 trp1-1 can1-100 leu2-3,112 his3-11,15 ura3-1 pan1:: PAN1-4-Myc-TRP1* (This study)
YMC514	*MAT* **a** *ade2-1 trp1-1 can1-100 leu2-3,112 his3-11,15 ura3-1 prk1Δ::HIS3 pan1:: PAN1-4-Myc-TRP1* (This study)
YMC515	*MAT a ade2-1 trp1-1 can1-100 leu2-3,112 his3-11,15 ura3-1 ark1Δ::LEU2 sla1:: Myc-SLA1-TRP1* (This study)
YMC516	*MAT a ade2-1 trp1-1 can1-100 leu2-3,112 his3-11,15 ura3-1 ark1Δ::LEU2 prk1Δ::HIS3 sla1:: Myc-SLA1-TRP1* (This study)
YMC506	*MAT* **a** *ade2-1 trp1-1 can1-100 leu2-3,112 his3-11,15 ura3-1 prk1Δ::HIS3 sla1:: Myc-SLA1-TRP1*

2.3. Oligonucleotide primers

Primers used for *E.coli*-co-expression kinase constructs:

LR1BamHF: 5'GTGTGGATCCATGTATAACCCGTACCAG3'

LR1EnStpR: 5'AGCACGAGCACGCTACTATTATGAGTTG ACAAAGCCAGTTGC3'

LR2BamHF:	5'GTGTGGATCCTTCATTACAGCGGGCGTAC 3'
LR2EnStpR:	5'AGCACGAGCACGCTACTATTAATTATTAAA GTTGGATTTGG3'
Sla1GST3BamHF:	5'GCTGGATCCGCAATGATGCCTTTGCAG3'
Sla1GST3EnStpR:	5'AGCACGAGCACGCTACTATTAGAATCCAAA CGGATTTGATG3'
EnhaF:	5'CGTGCTCGTGCTAATAATTTTGTTTAACTTT AAGAAG3'
ARK299HAR:	5'GGACGTCGTATGGGTACATAATTGATATCC TCTTCAG3'
EnhaPrkF:	5'CTTTAAGAAGGAGATATAATGAATACTCCA CAGATTAGTC3'
EnhaArkF:	5'CTTTAAGAAGGAGATATAATGAATCAACCT CAAATTGGC3'
PK298HAR:	5'GGACGTCGTATGGGTATAACCTGGAAACCT CCTC3'
HAxho1R:	5'GTGTCTCGAGAGCGTAGTCTGGGACGTCGT ATGGG3'

Primers for Ark1^{D159Y} Mutagenesis

Ark1orfAscF:	5'CGTGGCGCGCCGAATCAACCTCAAATTGGC3'
ArkD159YR:	5'CTATCTTTATATAACGGTGAATTAAC3'
ArkD159YF:	5'GTTAATTCACCGTTATATAAAGATAG3'
Ark1orfxhoR:	5'CGTCTCGAGTCACTTATCCAAGGATAAC3'

Primers for fusion of Ark1 kinase domain with Prk1 C terminal, and Prk1 kinase domain fusion with Ark1 C terminal

Ark1BamHF:	5'GCTGGATCCATGAATCAACCTCAAATTGG3'
ArkN299R:	5'CATAATTGATATCCTCTTCAG3'
Prk1C299F:	5'CTGAAGAGGATATCAATTATGCAGAATAAG CCTTGCCCG3'
PKorfAscR:	5'GTGTGGCGCGCCAACTTTGCTGGGAAACC3'
PrkorfXba1F:	5'GTGTCTAGAATGAATACTCCACAGATTAGT C3'
PrkN299R:	5'CACGGAACATTTTGCATCTGTAACCTGGAA ACCTCC3'
ArkC299F:	5' ATGCAAAATGTTCCGTGTCC3'
ArkorfAscR:	5'GTGGGCGCGCCCTTATCCAAGGATAACTTT CG3'

Primers for Prk1AR mutagenesis

ArkC299F:	5' ATGCAAAATGTTCCGTGTCC3'
PrkorfXba1F:	5'GTGTCTAGAATGAATACTCCACAGATTAGT C3'
PrkAF:	5'CAAGTGGTTCAGGCGCCCAGTAGCCATTTGA/ ACCCAATTGGCCGGTG3'
PrkAR:	5'GCGCCTGAACCACTTGTATGTCATTAATCG GGCAAGGCTTATTCTG3'
PKorfAscR:	5'GTGTGGCGCGCCAACTTTGCTGGGAAACC3'

Restriction site added is underlined. Additional residues were added 5' to the restriction site to facilitate complete restriction enzyme cleavage at the ends of PCR products.

2.4. Recombinant DNA methods

General recombinant DNA methods were performed essentially as described by Sambrook *et al.* (1989). Polymerase chain reaction (PCR) was carried out with Vent DNA polymerase. Restriction enzyme digestion was performed using the appropriate buffers supplied by the manufactures. Blunt ending of DNA fragments was carried out using Klenow DNA polymerase. Dephosphorylation of cloning vectors was done using calf intestinal phosphatase (CIP). T4 DNA ligase (New England Biolabs or Roche) was used for ligation of DNA fragments.

2.4.1. Transformation of *E. coli* cells

For heat shock transformation, DNA from ligation mix (7.5µl) or plasmid DNA (less than 0.1 µg) was mixed with 50 µl KCM buffer (100 mM KCl, 30 mM $CaCl_2$, 50 mM $MgCl_2$), and 100 µl of competent cells. After incubation on ice for 30-45 min, the cells were heat shocked at 43^{o}C water bath for 50 seconds. The transformed cells were quickly incubated on ice for at least 1 min before being plated out on the LB agar plates with appropriate antibiotics according to the selection marker of individual plasmid.

For electroporation transformation, combine 20 µl of the electro-competent cells with 1-2 µl of plasmid or ligation mixture in 0.2 cm electroporation cuvettes (Bio-rad) and leave on ice for 5 min. The electroporation was done using a Gene Pulser (Bio-Rad) at a voltage of 2 KV and with a resistance and capacitance of 200 Ω resistances and 25 µF, respectively. Following electroporation, cells were resuspended in 1 ml of LB and grown at 37°C for 1 h. Aliquots of the cells were

spread onto agar plates containing the selective medium with the appropriate antibiotics.

2.4.2. Plasmid preparation and analysis

Overnight bacterial culture (2.0 ml) was pelleted by centrifugation at full speed in table-top centrifuge for 30 sec. The resulting bacterial pellet was resuspended in 250 µl of STET buffer (8% sucrose, 0.5% Triton X-100, 50 mM Tris-HCI pH8.0, 50 mM EDTA, 1 mg/ml freshly prepared lysozyme). The mixture was boiled at 100^{o}C water bath for 2 min and subsequently centrifuged at full speed for 5 min. After removal of the bacterial debris by toothpicks, 250 µl of isopropanol was added to the supernatant, and the mixture was mixed by vortex before being centrifuged at full speed (13,000 rpm) for 10 min. The DNA pellet was washed with 70% ethanol and then dissolved in 50 µl of TE buffer (10 mM Tris-HCl, 1 mM EDTA, [pH8.0]) containing 0.1 µg/µl RNAase.

For high-quality plasmid DNA purification, QIAprep Miniprep Kit (QIAGEN Inc., Germany) was used and the procedure was according to the manufacturer's protocol.

• Spin down cells from a 5 ml overnight culture by centrifugation at full speed in an Eppendorf 5145c centrifuge (Eppendorf, Hamburg, Germany). Decant the supernatant and resuspend the cell pellet thoroughly in 250 µl of Buffer P1 (50 mM Tris-HCl, pH8.0; 10 mM EDTA; 100 µg/ml RNaseA). Transfer the cell suspension to a 1.5 ml microfuge tube.

• Lyse cells by adding 250 µl of Buffer P2 (200 mM NaOH, 1% SDS). Mix gently by inverting the tube several times.

• Add 350 µl of Neutralization Buffer N3 (3.0 M potassium acetate, pH5.5) and mix gently but thoroughly to prevent localized precipitation.

• Centrifuge at full speed in the Eppendorf centrifuge for 10 min to pellet the precipitated proteins and genomic DNA.

• Transfer the supernatant to the QIAprep column and centrifuge at full speed for 30-60 s. Discard the flow-through.

• Wash the column by adding 0.5 ml of Buffer PB and centrifuge at full speed for 30-60 s. Discard the flow-through.

• Wash column with 0.75 ml of Buffer PE and centrifuge for 30-60 s. Discard flow-through and centrifuge the column for 1 min to remove the residual wash buffer.

• Place the column in a fresh 1.5 ml microfuge tube. Add 50 µl of Buffer EB (10 mM Tris-HCl, pH 8.5) to the column; let it stand for 1 min before centrifugation to elute the DNA. Restriction digestions were performed to analyze the plasmid constructs. Normally, 1-2 µg of the plasmid DNA was digested with 1-2 units of the appropriate enzymes in a 20 µl reaction at 37°C for 2 h. The digestion products were analyzed by agarose gel electrophoresis.

Table 2. Plasmid Constructs Used in This Study

Construct	Description
pARK1-HA	*ARK1 coding* region was generated by PCR, cloned in frame with a C-terminal *HA* epitope followed by the *ADH1* terminator, and placed under *PRK1*promoter control in pRS316.

pPRK1-HA	*PRK1 coding region was generated by* PCR, cloned in frame with a C-terminal *HA* epitope followed by the ADH1 terminator, and placed under *PRK1* promoter control in pRS316.
pARK1n-PRK1c-HA	The DNA coding region for Ark1p (1-299a.a.) was fused with the DNA coding region for Prk1p (299-8109a.a.) by PCR, cloned in frame with a C-terminal *HA* epitope followed by the *ADH1* terminator, and placed under *PRK1* promoter control in RS316
pPRK1n-ARK1c-HA	The DNA coding region for Prk1p (1-298a.a.) was fused with the DNA coding region for Ark1p (300-639a.a.) by PCR, cloned in frame with a C-terminal *HA* epitope followed by the *ADH1* terminator, and placed under *PRK1* promoter control in RS316.
pPRK1$_{298}$-HA	The DNA coding region for Prk1p kinase domain (1-298 a.a.) was generated by PCR and cloned in frame with a C-terminal *HA* epitope followed by the *ADH1* terminator, and placed under *PRK1* promoter control in pRS316.
pPRK1Δpp-HA	The DNA coding region for Prk1p (1-747 a.a.) was generated by PCR and cloned in frame with a C-terminal *HA* epitope followed by the *ADH1* terminator, and placed under *PRK1* promoter control in pRS316.
pARK1Δpp-HA	The DNA coding region for Ark1p (1-606 a.a.) was generated by PCR and cloned in frame with a C-terminal *HA* epitope followed by the *ADH1* terminator, and placed under *ARK1* promoter control in pRS316.
pPRK1$_{319}$-HA	The DNA coding region for Prk1p (1- 319 a.a.) was generated by PCR and cloned in frame with a C-terminal *HA* epitope followed by the *ADH1* terminator, and placed under *PRK1* promoter control in pRS316.
pPRK1$_{AR}\Delta$pp-HA	The DNA coding region for Prk1p (1-747 a.a.) with Prk1p (299 to 319a.a.) replaced with Ark1p according region (300 to 320a.a.) was generated by PCR and cloned in frame with a C-terminal *HA* epitope followed by the *ADH1* terminator, and placed under *PRK1* promoter control in pRS316.
pPRK1$_{AR}$ -HA	The DNA coding region for Prk1p with Prk1p (299 to 319a.a.) replaced with Ark1p according region (300 to 320a.a.) was generated by PCR, cloned in frame with a C-terminal *HA* epitope followed by the A*DH1* terminator, and placed under PRK1 promoter control in pRS316.
pPAN1-Myc-304	The DNA coding region for Pan1p (1252-1480 aa) was

	generated by PCR and cloned in frame with a C-terminal *Myc* epitope followed by the A*DH1* terminator in pRS304.
pPAN1-Myc	*PAN1* open reading frame was generated by PCR and cloned in frame with a C-terminal *Myc* epitope followed by the *ADH1* terminator, and placed under *PAN1 promoter* control in pRS314.
pMyc-SLA1-304	Myc-Sla1p. *SLA1* open reading frame was generated by PCR and cloned in frame after three copies of the Myc epitope, under *SLA1* promoter control in pRS304.
pMyc-SLA1	Myc-Sla1p. *SLA1* open reading frame was generated by PCR and cloned in frame after three copies of the Myc epitope, under *SLA1* promoter control in pRS314.
pGADT7-ARP2	*ARP2* coding region was generated by PCR and cloned in frame into pGADT7.
pGBKT7-ARP2	*ARP2* coding region was generated by PCR and cloned in frame into pGBKT7.
pGBKT7-PRK1^{D158Y}	The coding region of Prk1^{D158Y}p was generated by PCR and cloned in frame into pGBKT7 (Zeng et al. 2001).
pGBKT7-PRK1 $^{D158Y}_{(1-747)}$	The DNA coding region of Prk1^{D158Y}p (1-747 a.a.) was generated by PCR and cloned in frame in pGBKT7.
pGBKT7-PRK1 $^{D158Y}_{(1-319)}$	The DNA coding region of Prk1^{D158Y}p (1-319 a.a.) was generated by PCR and cloned in frame in pGBKT7
pGADT7-PRK1$^{D158Y}_{298}$	The DNA coding region for Prk1p (1-298 a.a.) was generated by PCR and cloned in frame into pGADT7.
pGEX-SR	GST-SR; The DNA coding region for Sla1p (1068-1244 a.a.) was generated by PCR and cloned in frame into pGEX-4T-1.
pGEX-SR-ARK1$_{299}$HA	For GST-SR and ARK1299-HA co-expression in E. Coli. The DNA coding region for Sla1p (1068-1244 a.a.) followed by three stop codons, was fused with a translational enhancer, a Shine-Dalgarno sequence and Ark1p kinase domain coding region(1-299a.a.) followed with a HA tag at C-terminal by PCR fusion method, and cloned into the BamHI and XhoI sites of pGex-4T-1.
pGEX-SRmut-ARK1$_{299}$HA	For GST-SRmut and ARK1$_{299}$-HA co-expression in E. Coli. GST-SRmut is GST-SR variant with all TG to AG mutations.
pGEX-SR-ARK1$^{D159Y}_{299}$HA	For GST-SR and ARK1$^{D159Y}_{299}$-HA co-expression in E. Coli. ARK1^{D159Y}299-HA is ARK1$_{299}$-HA variant with D159Y mutation.

pGEX-SR-PRK1$_{298}$-HA	For GST-SR and PRK1^{298}-HA co-expression in E. Coli. The DNA coding region for Sla1p (1068-1244 a.a.) followed by three stop codons, was fused with a translational enhancer, a Shine-Dalgarno sequence and Prk1p kinase domain coding region(1-298a.a.) followed with a HA tag at C-terminal by PCR fusion method, and cloned in frame into the BamHI and XhoI sites of pGex-4T-1.
pGEX-LR1-ARK1$_{299}$-HA	For GST-LR1 and ARK1$_{299}$-HA co-expression in E. Coli. The DNA coding region for Pan1p (1-245 a.a.) followed by three stop codons, was fused with a translational enhancer, a Shine-Dalgarno sequence and Ark1p kinase domain coding region(1-299a.a.) followed with a HA tag at C-terminal by PCR fusion method, and cloned in frame into pGex-4T-1.
pGEX-LR1-ARK1$^{D159Y}{}_{299}$-HA	For GST-LR1 and ARK1$^{D159Y}{}_{299}$-HA co-expression in E. Coli. ARK1$^{D159Y}{}_{299}$-HA is ARK1$_{299}$-HA variant with D159Y mutation.
pGEX-LR1-PRK1$_{298}$-HA	For GST-LR1 and PRK1298-HA co-expression in E. Coli. The DNA coding region for Pan1p (1-245 a.a.) followed by three stop codons, was fused with a translational enhancer, a Shine-Dalgarno sequence and Prk1p kinase domain coding region(1-299a.a.) followed with an HA tag at C-terminal by PCR fusion method, and cloned into the BamHI and XhoI sites of pGEX-4T-1.
pGEX-LR2-ARK1$_{299}$-HA	For GST-LR2 and ARK1$_{299}$-HA co-expression in E. Coli. The DNA coding region for Pan1p (384-584 a.a.) followed by three stop codons, was fused with a translational enhancer, a Shine-Dalgarno sequence and Ark1p kinase domain coding region (1-299a.a.) followed with an HA tag at C-terminal by PCR fusion method, and cloned into the BamHI and XhoI sites of pGEX-4T-1.
pGEX-LR2-ARK1$^{D159Y}{}_{299}$-HA	For GST-LR2 and ARK1$^{D159Y}{}_{299}$-HA co-expression in E. Coli. ARK1$^{D159Y}{}_{299}$-HA is ARK1$_{299}$-HA variant with D159Y mutation.
pGEX-LR2-PRK1$_{298}$-HA	For GST-SR and ARK1$_{299}$-HA co-expression in E. Coli. The DNA coding region for Pan1p (384-584 a.a.) followed by three stop codons, was fused with a translational enhancer, a Shine-Dalgarno sequence and Prk1p kinase domain coding region(1-298a.a.) followed with an HA tag at C-terminal by PCR fusion method, and cloned in frame into the BamHI and XhoI sites of pGEX-4T-1.
pGAL-HA-PRK1	The *PRK1* coding region was generated by PCR, cloned in frame with the *HA* epitope, and placed under *GAL1* promoter control in pRS316 (Zeng and Cai, 1999).

pGAL-HA-ARK1	The *ARK1* coding region was generated by PCR, cloned in frame with the *HA* epitope, and placed under *GAL1* promoter control in pRS316.
pGAL-HA-ARK1^{D159Y}	The *ARK1* coding region was generated by PCR, cloned in frame with the *HA* epitope, and placed under *GAL1* promoter control in pRS316.
pGAL- PRK1^{D158Y}-EGFP	*PRK1 ^{D158Y}* coding region was generated by PCR, cloned in frame with a C-terminal *EGFP* epitope followed by the *ADH1* terminator, and placed under *GAL1* promoter control in pRS316.
pGAL- PRK1$^{D158Y}{}_{319}$-EGFP	The DNA coding region for Prk1^{D158Y}p (1-319a.a.) was generated by PCR, cloned in frame with a C-terminal *EGFP* epitope followed by the *ADH1* terminator, and placed under *GAL1* promoter control in pRS316.
pGAL- PRK1$^{D158Y}{}_{298}$-EGFP	The DNA coding region for Prk1^{D158Y}p (1-298a.a.) was generated by PCR, cloned in frame with a C-terminal *EGFP* epitope followed by the *ADH1* terminator, and placed under *GAL1* promoter control in pRS316.
pGAL- PRK1$^{D158Y}{}_{AR}$-EGFP	The DNA coding region for Prk1^{D158Y}p with Prk1p (299 to 319a.a.) replaced with Ark1p according region (300 to 320a.a.) was generated by PCR, cloned in frame with a C-terminal *EGFP* epitope followed by the *ADH1* terminator, and placed under *GAL1* promoter control in pRS316.
pGAL-PRK1$^{D158Y}{}_{AR}$Δpp-EGFP	The DNA coding region for Prk1^{D158Y}p (1-747 a.a.) with Prk1p (299 to 319a.a.) replaced with Ark1p according region (300 to 320a.a.) was generated by PCR, cloned in frame with a C-terminal *EGFP* epitope followed by the *ADH1* terminator, and placed under *GAL1* promoter control in pRS316.
pGAL-PRK1$^{D158Y}{}_{AR}$Δpp-Myc	The DNA coding region for Prk1^{D158Y}p (1-747 a.a.) with Prk1p(299 to 319a.a.) replaced with Ark1p according region (300 to 320a.a.) was generated by PCR, cloned in frame with a C-terminal *Myc* epitope followed by the *ADH1* terminator, and placed under *GAL1* promoter control in pRS316.
pGAL-PRK1^{D158Y}Δpp-Myc	The DNA coding region for Prk1^{D158Y}p (1-747 a.a.) was generated by PCR, cloned in frame with a C-terminal *Myc* epitope followed by the *ADH1* terminator, and placed under *GAL1* promoter control in pRS316.
pGEX-PRK1$_{319}$	GST-PRK1$_{319}$; The DNA coding region for Prk1p (1-319 a.a.) was generated by PCR and cloned in frame into pGEX-6p-1.

pGEX-PRK1$_{298}$	GST-PRK1$_{298}$; The DNA coding region for Prk1p (1-298 a.a.) was generated by PCR and cloned in frame into pGEX-6p-1.
pET-ARP2	His-ARP2; *ARP2* coding region without intron was generated by PCR and cloned in frame into pET-Duet-1.
ARP2-HA-305	The DNA coding region for Arp2p with *ARP2* promoter was generated by PCR and cloned in frame with a C-terminal *HA* epitope followed by the *ADH1* terminator in pRS305.
pARK1$_{PR}$-HA	The DNA coding region for Ark1p with Ark1p (300 to 320a.a.) replaced with Prk1p according region (299 to 319a.a.) was generated by PCR, cloned in frame with a C-terminal *HA* epitope followed by the ADH1 terminator, and placed under ARK1 promoter control in pRS316.
pPAN1-4-Myc-304	The DNA coding region for Pan1p (1-849aa) was generated by PCR and cloned in frame with a C-terminal *Myc* epitope followed by the *ADH1* terminator in pRS304.
pGBKT7-ARK1 $^{D159Y}{}_{PR}$	The DNA coding region of Ark1^{D159Y}p, with Ark1p (300 to 320a.a.) replaced with Prk1p according region (299 to 319a.a.) was generated by PCR and cloned in frame into pGBKT7.

2.4.3. Mutagenesis

Mutations in pGEX-SRmut-ARK1$_{299}$HA, Ark1^{D159Y}, Prk1$_{AR}$HA-316 were generated either by one step PCR with mutagenic primers or by sequential PCR mutagenesis as described (Cormack and Somssich, 1997), and confirmed by sequencing analysis.

2.5. Yeast manipulations

Yeast genetic techniques were performed according to standard methods described previously (Rose, 1990).

2.5.1. Yeast transformation

The host cells were grown in appropriate medium to the log phase and harvested by centrifugation at 3000 rpm for 5 min. For each transformation, about 50 µl of the cell pellet was washed once in Li-TE buffer (0.1 M lithium acetate, 10 mM Tris-HCl pH 7.5, 1 mM EDTA), and resuspended in 100 µl of yeast transformation mix (2 M LiAc : 50% PEG 8000 : 1 M DTT = 1:8:1). The cell suspension was then mixed with the plasmid DNA and 10 µl of salmon sperm carrier DNA (9.5 µg/µl salmon testes DNA, Sigma) followed by incubation at 42°C for 30 min. The cells were collected by centrifugation at low speed and resuspended in 1 ml of H_2O. The cell suspension was spread onto selective plates and incubated at the appropriate temperature for 3 to 4 days.

2.5.2. Preparation of yeast genomic DNA

To extract genomic DNA from yeast, the cells were grown in 2.5 ml proper medium and proper temperature overnight. 2ml cells were centrifuged at high speed for 5 seconds. Cell pellet was resuspended in 160µl 1M sorbitol, 0.1M EDTA (pH7.5), and transferred to 1.5 ml tube. 40µl lyticase (10mg/ml) and 1.6µl β-mercaptoethanol were added to the reaction tube. Reaction tubes are place on the roller wheel at 30ºC for 1 hour. The cells were centrifuged at high speed for 30 seconds, and the supernatant discarded. The cell pellet was resuspended in 250 µl 50mM Tris (pH7.4), 20mM EDTA. 25µl 10% SDS was added, mixed well and incubated at 65ºC, for 15 min. 100 µl 5M KAc was added, vortexed, and put on ice for 15 min. After spinning at high speed for 5 min, supernatant was

transferred to a new tube, and 350 µl (equal volumn) isopropanol added, mixed well and then held at room temperature for 5 min. After another high speed centrifugation and supernatant was discard. The pellet was wash with 900µl 70% Ethanol, spun at high speed for 1 min and the ethanol decanted, and the pellet dried. The pellet was dissolved in 50 µl TE (pH7.4), 5 µl RNase A (10 mg/ml). 2 µl of DNA was taken for subsequent PCR analysis.

2.5.3. Gene integration and PCR conformation

To obtain YMC501, YMC502, YMC503 and YMC509, plasmid pPAN1-Myc-304 was linearized within the *PAN1* gene by *BamHI* digestion and integrated into W303-1A, YMC410, YMC411, YMC414, respectively. To obtain YMC505, YMC506, and YMC507, plasmid pMyc-SLA1-304 was linearized within the *SLA1* gene by *BamHI* digestion and integrated into W303-1A, YMC410, YMC411, respectively. To obtain YMC510, plasmid Arp2-HA-305 was linearized within the *ARP* gene promoter by BspEI digestion and integrated into W303-1A. The integration was confirmed by PCR (Huxley *et al.*, 1990) and sequencing analysis.

2.6. Microscopy and fluorescence studies

2.6.1. Rhodamine phalloidin staining

Staining of actin filaments with rhodamine-phalloidin (Molecular Probes, Eugene, OR) was performed as described previously (Adams and Pringle, 1991) with minor modifications. Cells were grown in at 25ºC in Ura dropout with raffinose as the carbon source medium to early log phase, and galactose was later

added for *GAL1* induction. After 1 hour galactose induction, cells were colleted and suspended in fixation solution (3.7% formaldehyde, 100 mM KH2PO4, 100 mM K2HPO4) for 45 min. Cells were then washed two times with PBS and suspended in PBS containing 0.1% Triton X-100 for 15 min. After washing again with PBS for two times, cells were incubated with PBS containing rhodamine-phalloidin (1:500) at 25ºC for 30 min. Cells were finally washed with PBS for four times and suspended in Vectashield mounting medium, and followed by visualization with the Leica DMAXA microscope.

2.6.2. Lucifer Yellow uptake assay

Cells were grown in 25 ml of YEPD or selection medium at 24ºC overnight with shaking. When cell density was 0.7-1.0 X 10^7 cells/ml, 1 ml of cell culture was placed in a 1.5 ml tube with punctures. Cells were gently pelleted in labtop centrifuge at 13,000 rpm for 1 minute at room temperature. After removing the supernatant, the cell pellet was resuspended in 90 µl of fresh YEPD. 10 µl of freshly prepared Lucifer Yellow stock solution (Dilithium salt) was added and incubated at 24 ºC for 2 hours. 1 ml ice-cold wash buffer (50mM Na_2HPO_4/NaH_2PO_4 pH 7, 10mM NaF, 10mM Na azide) was added to the reaction tube to stop the reaction and immediately put sample on ice. The cells were washed with ice cold wash buffer 3 times, suspended in Vectashield mounting medium, and followed by visualization with the Leica DMAXA microscope.

2.7. Protein studies

2.7.1. Yeast protein extraction

To prepare crude protein extracts using acid-washed glass beads, yeast strains were grown in appropriate conditions to mid-log phase (OD_{600} = 0.9 to 1.2). Cells were harvested, washed once with Stop mix buffer (0.9% NaCl, 1 mM NaN_3, 10 mM EDTA, 50 mM NaF) and resuspended in 200 µl of ice-cold lysis buffer (1% Triton X-100, 0.1% SDS, 100 mM NaCl, 50 mM Tris-HCl [pH7.2], 1 mM PMSF, 20 µg/ml leupeptin, 40 µg/ml aprotinin, 0.1 mM Na-orthovanadate, 15 mM p-nitrophenyl phosphate (PNPP)). 200 µl of acid-washed 500-µm-diameter glass beads (Sigma) were added to the cell suspension and the cells were lysed by vortexing vigorously at 4°C. After two rounds of high speed centrifugation to pellet out the cellular debris, the supernatant containing the crude cell lysate was collected, snap frozen in liquid nitrogen and stored at -80°C. Protein concentration was determined using the Coomassie Plus-200 Protein Assay Reagent (PIERCE, U.S.A). Crude protein extraction prepared by this way can be used for immunoprecipitation.

To prepare total protein extracts by TCA precipitation, 1 ml cells equivalent to OD_{600} = 4 were harvested by centrifugation and resuspended in 300 µl ice-cold water. Then, 150 µl of YEX lysis buffer (1.85 M NaOH, 7.5% β-mercaptoethanol) was added and the suspension was kept on ice for 10 min. Subsequently, 150 µl of 50% ice-cold TCA was added to the suspension which was further kept on ice for another 10 min. The precipitate was collected by centrifugation at 4°C for 5 min and then resuspended in a solution containing 35

μl of two times SDS-loading buffer (100 mM dithiothreitol, 50 mM Tris-HCl [pH 6.8], 2% SDS, 0.1% bromophenol blue, 10% glycerol) and 15 μl 1 M Tris buffer [pH 8.0]. After boiling for 10 min, 5 to 10 μl of each samples were loading on an SDS-PAGE, and used for subsequent analysis.

2.7.2. Immunoprecipitation and Western blot

Yeast cells were grown at 30°C to mid-log phase (*A*600 = 0.9 to 1.2) in 150 ml of SC medium lacking the appropriate amino acids, washed once in solution A (0.9% NaCl, 1 mM NaN3, 10 mM EDTA, 50 mM NaF), and resuspended in 900 μl of solution B (1% Triton X-100, 1% sodium deoxycholate, 0.1% sodium dodecyl sulfate [SDS], 50 mM Tris-HCl [pH 7.2], 100 mM sodium orthovanadate, 15 mM *p*-nitrophenylphosphate, 1 mM phenylmethylsulfonyl fluoride, protease inhibitors). Cells were then lysed at 4°C by vortexing with 500-μm-diameter acid-washed glass beads (Sigma). After centrifugation at 15,000 *g* for 20 min, the supernatant was transferred to a new tube and the protein concentration was measured. For immunoprecipitation, cell lysates (about 3 mg) were incubated for 1 h at 4°C with mouse anti-HA antibody or with mouse monoclonal anti-Myc antibody, respectively, to precipitate HA-tagged and Myc-tagged proteins. The mixture was incubated on ice for 1 hour, and followed by the incubation with Protein A/G PLUS-Agrose beads (Santa Cruz Biotechnology, pre-equilibrated in lysis buffer with protease inhibitors) for another 1 at 4°C with gentle agitation. The beads were then washed 4 times in RIPA buffer (1% Triton X-100, 150 mM NaCl, 50 mM Tris-HCl [pH 7.2]). The immune complexes were released by boiling in sample buffer for 5 min. After centrifugation, samples were loaded on

SDS–7.5 or 10% polyacrylamide gels. After electrophoresis, the separated proteins were electroblotted onto Immobilon-P membranes (Millipore).

SDS-polyacrylamide gel electrophoresis (SDS-PAGE) was performed using the Mini-PROTEIN II electrophoresis cell (Bio-Rad, USA). The separation gel contained 8% to 12% of acrylamide mix (acrylamide:bisacrylamide, 29:1), 375 mM Tris-HCI [pH8.8] and 0.1% SDS. The stacking gel contained 5% acrylamide mix, 125mM Tris-HCl [pH6.8] and 0.1% SDS. Polymerization was induced by the addition of TEMED and freshly prepared ammonium persulfate. Protein samples in SDS-loading buffer were boiled for 8 min, and loaded onto the gel. The electrophoresis was carried out in Tris-glycine buffer (25 mM Tris, 250 mM glycine, 0.1% SDS). The prestained broad range protein marker (New England Biolabs) was used to estimate the size of proteins.

After electrophoresis, the separated proteins were electro-transferred onto Immobilon PVDF membranes (Millipore, USA) using the liquid transfer cell (Bio-Rad, USA). The transfer buffer contained 3.30 g/L Tris and 14.4 g/L glycine. For Western blot, the membrane was incubated overnight at 4°C in blocking solution (PBS containing 0.05% Tween-20 and 5% skimmed milk). The membrane was sequentially incubated with the primary antibody and the HRP-conjugated secondary antibody, and followed by extensive wash with PBS containing 0.05% Tween-20. The antibody-antigen complexes were visualized with the Enhanced Chemiluminescence (ECL) system (Amersham, UK).

To treat the immunoprecipitates with calf intestinal alkaline phosphatase (CIP), the protein A-Sepharose beads were washed with RIPA buffer (50 mM Tris-HCl, pH 7.2, 1% Triton X-100, 1% sodium deoxycholate, 0.1% SDS, 150

mM NaCl), followed by incubation at 37 ºC with 1ml of 10 U/ml CIP (Biolabs, Inc.) for 30 min and boiling in the sample buffer.

2.7.3. GST fusion protein purification

To make GST-fusion proteins, the DNA coding regions were obtained by PCR and cloned in frame to a bacterial GST expression vector pGEX-4T-1 (Amersham Pharmacia Biotech, Malaysia). The plasmids were transformed into *E. coli* strain BL21.

Transformants were grown to OD_{600} = 0.7 in 200 ml of Luria-Bertani(LB) medium containing 100 mg of ampicillin (Sigma) per ml , and induced with 1 mM isopropylthioβ-D-galactoside (Life Technologies, Inc.) at 30ºC for 6 hours to express the fusion proteins. Cells were collected by centrifugation (GSA, Beckman), and resuspended in cold PBS buffer. The suspensions were sonicated on ice to lyse the cells and the lysates were centrifuged at 10,000 rpm for 10 min in a Sorvall SS-34 rotor. The supernatants were incubated with glutathione - Sepharose 4B beads (Pharmacia) for 30 min at room temperature, then transferred to disposable columns (Pharmacia). The beads were washed with PBS three times and the fusion proteins were eluted from the beads by incubation with elution buffer (10 mM glutathione, 50 mM Tris-HCl, pH 8.0) at 24ºC for 20min.

2.7.4. *E.coli* co-expression kinase assay

The bi-cistronic expression plasmids for *E. coli* co-expression assay were generated as follows (Figure2.1). The DNA coding region for the substrates (SR,

SRmut, or LR1, LR2) followed with 3 stop codons, a translational enhancer and a Shine-Dalgarno sequence (5'CGTGCTCGTGCTAATAATTTTGTTTAACTT TAAGAAGGAGATATA3'; Tan, 2001), were fused with kinase (Ark1p kinase domain or Prk1 kinase domain followed with an HA tag at C-terminal) by PCR fusion method, then cloned in frame into the BamHI and XhoI sites of pGEX-4T-1 (Amersham Biosciences, Singapore).

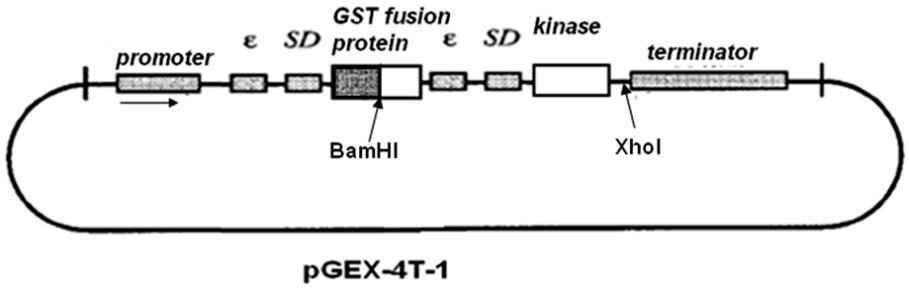

Figure 2.1 The bi-cistronic expression plasmids construction for *E. coli* co-expression assay.

The coding regions of the substrates (SR, SRmut, or LR1, LR2) followed by 3 stop codons, a translational enhancer and a Shine-Dalgarno sequence (5'CGTGCTCGTGCTAATAATTTTGTTTAACTTTAAGAAGGAGATATA 3', Tan, 2001), were fused to the kinase domains of either Ark1p or Prk1p (containing an HA tag at the C-termini) by PCR, and then cloned in frame into the BamHI and XhoI sites of pGEX-4T-1 (Amersham Biosciences).

The bi-cistronic expression plasmids were transformed into *E. coli* strain BL21, and the transformants were grown in 200 ml of Luria-Bertani medium containing 100 mg of ampicillin (Sigma) per ml to an optical density at 600 nm of 0.8. The expression of GST fusion proteins and HA tagged kinases were induced with 1 mM isopropyl-1-thio-b-D-galactopyranoside (IPTG) (Life Technologies, Inc.) at 30°C for 1hour. The subsequent purification of the GST fusion substrate proteins were performed as described above. The expression of

kinases was confirmed first by analysis of the cell lysates by 10% SDS-PAGE and western. Then the purified GST-fusion substrates were subjected to the 10% SDS-PAGE and Western blotting to analyze the phosphothreonine modification status. The nitrocellulose membranes with electroblotted GST fusion substrates were later stained with Coomassie blue dye to visualize the GST fusion proteins.

2.7.5. His fusion protein purification and in vitro binding

Plasmid containing His-ARP2 was transformed into *E.coli* strain BL21 Gold (Stratagene). Transformants were grown in 200ml of ampicillin containing LB medium at 37ºC OD_{600} = 1.0, followed by the addition of IPTG to 1mM and incubation at 30 ºC for overnight. Cells were collected by centrifugation and resuspended in cold extraction buffer (1% Triton, 150mM NaCL, 5mM Imidazole, 20mM Tris-HCl, 1mMPMSF, pH8.0). The resuspended cells were sonicated on ice and the lyastes were centrifuged at 17,000 rpm for 20min. The supernatants were incubated with pre-washed Ni-NTA Agrose (QIAGEN, Germany), for 1 hour at 4 ºC. Then the beads were washed with wash buffer (150mM NaCl, 20mM Imidazole, 20mM Tris-HCl, 1mM PMSF, pH8.0) for 3 times. The His tagged proteins bound on Ni-NTA beads were eluted by incubating the beads with elution buffer (20mM Tris-HCl, 200mM NaCl, 250mM Imidazole).

For GST fusion protein binding experiments, 400 µl of approximately 3 mg of purified His-tag proteins was incubated with GST fusion protein coupled beads for 1hour at 4 ºC, washed five times with RIPA buffer, and then eluted into SDS-PAGE sample buffer.

2.7.6. In vitro kinase assay

For in vitro kinase assays, the yeast cells with GAL-HA-Prk1, Gal –HA-Ark, or Gal-HA-Ark1^{D159Y} were cultured in raffinose as the carbon source medium to early log phase, and galactose was later added for *GAL1* induction. After 3 hour galactose induction, cells were colleted. The cell extraction and IP was done as described. The polyclonal rabbit anti-HA antibody conjugated beads (Research Biolab) was used to precipitate HA-tagged Prk1p and HA-tagged Ark1p. The beads were first washed with the RIPA buffer for five times, then three times with 25 mM MOPS (pH 7.2) and resuspended in 6µl of HBII buffer (60 mM b-glycerophosphate, 25 mM MOPS, pH 7.2, 15 mM *p*-nitrophenylphosphate, 15 mM $MgCl_2$, 5 mM EGTA, 1 mM dithiothreitol, 1 mM phenylmethylsulfonyl fluoride, 20mg leupeptin/ml, and 0.1 mM sodium orthovanadate). The kinase assay was performed by incubating the beads with 5mg of GST-fusion proteins, 0.5µl of 1 mM ATP, 0.5µl of [γ-32P]ATP (10 mCi/ml; New England Nuclear Inc.), 1ml of 250 mM MOPS in a total volume of 20ml at 25ºC for 15min. The reaction was stopped by addition of protein gel sample buffer; the reaction mixture was denatured at 100ºC for 5 min, and subjected to 10% SDS-PAGE. The gels were first stained with Coomassie blue to visualize the protein bands. After pictures were taken, the gels were fixed, dried, and exposed to x-ray films.

2.7.7. Co-Immunoprecipitation

Co-Immunoprecipitation of Prk1p and Arp2p was done as described (Lechler *et al.*, 2000) with some modifications. Briefly, Gal-Prk1$^{D158Y}{}_{AR}$Δpp-Myc or Gal-

Prk1^{D158Y}Δpp-Myc was transformed into cells with Arp2-HA. The resultant strains were grown at 30ºC with raffinose as the carbon source medium to early log phase, and galactose was later added for *GAL1* induction. After 1 hour galactose induction, cells were colleted. The cell extraction and IP was done as described (Lechler *et al.*, 2000). The cell lysate was centrifuged at 300,000 *g* for 60 min. The resulting high-speed supernatant was nearly at a concentration of ~10 mg/ml. 40 µl high-speed extract was incubated, for 1 h at 4°C, with 20 µl goat-anti Myc condjugated beads (NEB). Eluted proteins were precipitated with 10% trichloroacteic acid and resuspended in protein gel sample buffer. Samples were separated by 10% PAGE and subsequent western blot analysis.

2.8. Yeast Two Hybrid Assay

The MATCHMAKER system (Clontech Laboratories, USA) was used in two-hybrid analysis. For the yeast two-hybrid assay, DNA fragments of *ARP2* and *PRK1^{D158Y}* were fused to the HA-tagged *GAL4* activation domain of pGADT7 or the Myc-tagged DNA binding domain of pGBKT7 as indicated in Table 2. Plasmids were co-transformed into the strain SFY526 and the expression of each fusion protein was confirmed by Western blotting with the use of anti-HA or anti-Myc antibodies. The β-galactosidase activities were measured as instructed by the manufacturer (CLONTECH, Palo Alto, CA).

Chapter 3

Identification of Ark1p substrates

3.1. Background

Endocytosis is a dynamic process which involves tightly controlled assembly and disassembly of endocytic coat components and actin networks throughout cargo capture, membrane invagination, vesicle scission and targeting. In yeast, one of the best characterized regulatory mechanisms of this process is the reversible phosphorylation of endocytic coat complex and actin filament assembly by members of Ark/ Prk kinase family.

Prk1p is the most extensively studied member of Ark/Prk kinase family. It was isolated from a genetic screening of extragenic suppressors of an endocytic defective mutant *pan1-4* (Zeng and Cai, 1999) in yeast. A number of endocytic proteins, including Pan1p, Sla1p, Scd5p, Yap1801/2p and Ent1/2p, were identified as substrates of Prk1p (Zeng *et al.*, 2001; Watson *et al.*, 2001; Huang *et al.*, 2003; Henry *et al.*, 2003), and the Prk1p consensus phosphorylation motifs were identified as (L/I/V/M)xx(Q/N/T/S)xTG (Huang *et al.*, 2003).

Ark1p, another yeast member of this kinase family, was identified through a two hybrid screening for binding proteins of Sla2p (Cope et al., 1999). Ark1p shares high homology with Prk1p in the kinase domain (73% identical). The role of Ark1p overlaps with that of Prk1p, because neither *ark1* nor *prk1* single mutant shows actin cytoskeleton and endocytic defects; while in the absence of both kinases, the defects of actin cytoskeleton and endocytosis are striking (Cope *et al.*, 1999; Sekiya-Kawasaki *et al.*, 2003). However, the function of Ark1p has been barely studied, and its substrate and phosphorylation motifs are not clear.

Zeng et al. showed that Sla1p and Pan1p immunoprecipitated from *prk1*Δ were phosphorylated when incubated with radioactive ATP, whereas the two

proteins immunoprecipitated from *ark1*Δ *prk1*Δ cells could not be phosphorylated. It suggested that Ark1p may be the kinase which is co-precipitated with and phosphorylate Sla1p and Pan1p in vitro (Zeng et al., 2001). However, the direct evidence that Ark1p can phosphorylate these two proteins has not been reported. Later, Henry et al. tested Ark1p's kinase activity on synthetic peptides in vitro, and showed that Ark1p could phosphorylate AxTG motif instead of TxTG motif, which could be readily phosphorylated by Prk1p and Akl1p. But, there is only one AxTG motif present in Sla1p and no AxTG motif in Pan1p. So the Ark1p substrates and phosphorylation motifs remain unclear.

In order to understand how Ark1p functions in endocytic regulation, we began by studying Ark1p kinase activity and identifying Ark1p substrates.

3.2. Results

3.2.1. Kinase activity of Ark1p in a traditional kinase assay

As Ark1p and Prk1p are functionally redundant, it is reasonable to hypothesize that at least some of the substrates of Prk1p are expected to be shared by Ark1p. Sla1p, one of the known substrates of Prk1p, was first used as a potential substrate to test the kinase activity of Ark1p by the *in vitro* kinase assay. The Sla1p C-terminal region containing multiple Prk1p phosphorylation motifs was expressed as a GST fusion protein (named as GST-SR) and purified from *E. coli* for use in the kinase assay. To prepare the kinases, HA tagged Ark1p, as well as HA-Prk1p and HA-Ark1^{D159Y}p, were expressed under the inducible *GAL* promoter in yeast cells, immunoprecipitated and subjected to the in vitro kinase

assay. Ark1^{D159Y} is an Ark1 kinase mutant, in which the conserved Aspartic Acid in the catalytic domain of the kinase was mutated into tyrosine.

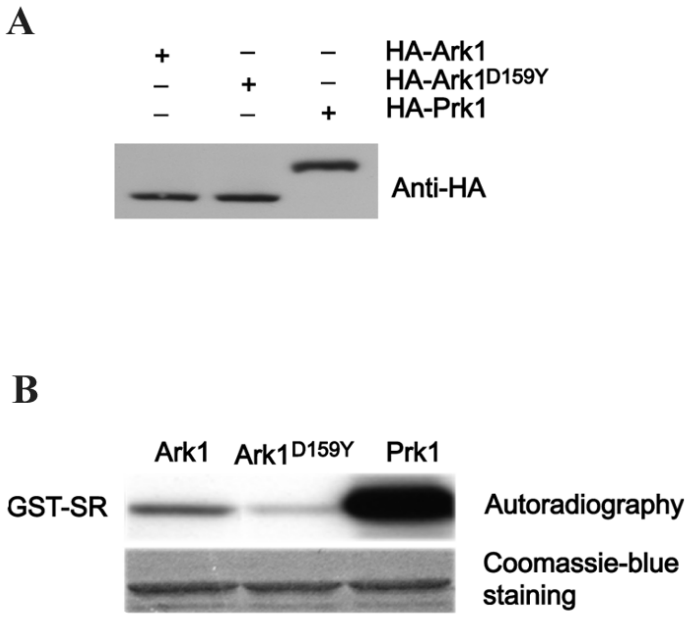

Figure 3.1 *In vitro* phosphorylation of Sla1p by Ark1p.

A. Wild-type Ark1p, the kinase-inactivated Ark1^{D159Y}p, and wild-type Prk1p were expressed as HA-tagged proteins and quantified by immunoprecipitation and western. Equal amounts of the immunoprecipitated proteins were used in the kinase reactions.

B. Phosphorylation results were shown as autoradiography and the input substrates were visualized by the coomassie blue staining.

The immunoprecipitated kinases were examined by SDS-PAGE and western blot to confirm the expression of the kinases. Equal amount of kinases are used in *in vitro* kinase assay (Figure 3.1 A). GST-SR was readily phosphorylated by

immunoprecipitated HA-Prk1p, as has been reported previously (Zeng *et al.*, 2001) (Figure 3.1 B, the third lane). HA-Ark1p prepared in the same way could also phosphorylate GST-SR, albeit much less effectively (Figure 3.2 B, the first lane). The $Ark1^{D159Y}$ mutant exhibited a largely abolished activity (Figure 3.1 B, the second lane).

3.2.2. Kinase activity of Ark1p in *E.coli* co-expression assay

To investigate whether the above result was due to an intrinsic low activity of Ark1p or to a suboptimal assay condition, the kinase activity was tested in a bacterial co-expression system. This system has been used successfully to establish the kinase activity of SRPK1 over its substrate ASF/SF2 (Yue *et al.*, 2000), and to test the effect of phosphorylation on protein interactions (Shaywitz *et al.*, 2002). GST fusion proteins were co-expressed with kinase by using a bi-cistronic expression vector (Figure 2.1). After induction, GST fusion proteins were purified and analyzed by the SDS-PAGE and western blot using anti phosphor-threonine antibody to detect the phosphorylation of the GST fusion proteins. GST-SR was co-expressed with the HA-tagged kinase domain of Ark1p, $Ark1^{D159Y}$ or Prk1p. The expression of the kinases was confirmed by immunoblotting with anti-HA antibody to be at similar levels (Figure 3.2A). As shown in Figure 3.2B, GST-SR co-expressed with either Ark1p or Prk1p kinase domain became equally extensively phosphorylated, whereas no phosphorylation could be detected when co-expressed with $Ark1^{D159Y}$ (Figure 3.2B, upper panel).

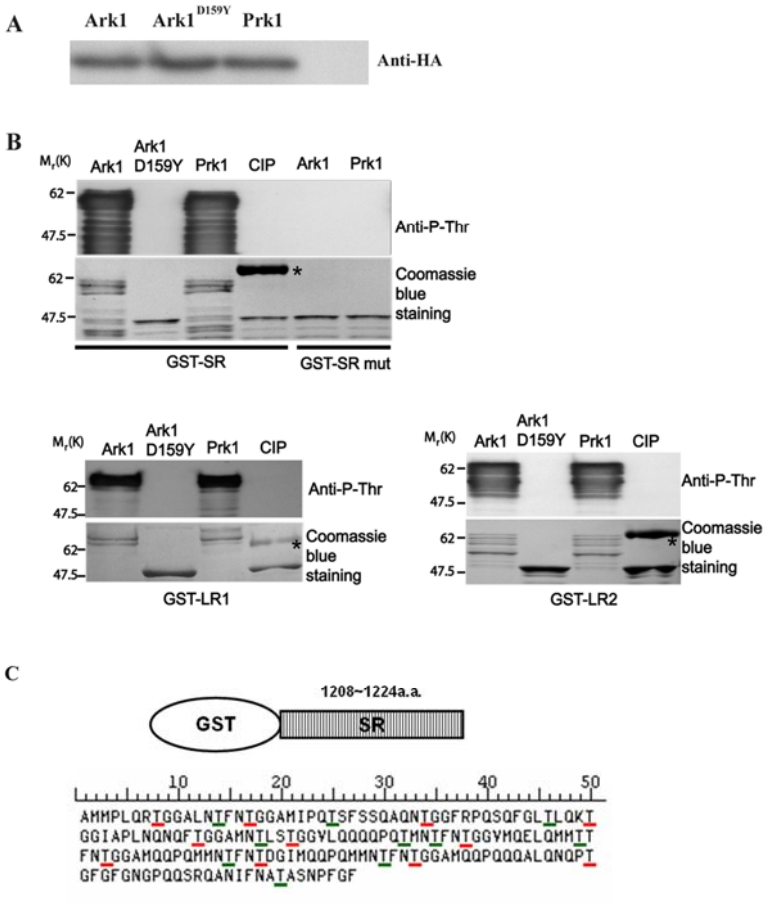

Figure 3.2 Phosphorylation of Sla1p-SR, Pan1p-LR1 and Pan1p-LR2 by Ark1p and Prk1p in *E. Coli.*

A. Expression of Kinases in the *E. Coli* co-expression system. The expression levels of kinases in the co-expressed *E.Coli* cells were examined by using antibody against HA antibody on immunoblots of cell extracts. Control is the cell transformed with pGEX-4T-1 vector.

B. GST fusion substrates, indicated below the panels, co-expressed with respective kinases, indicated above the panels, were purified after 1 h induction and analyzed by SDS-PAGE and Western. Lane 4 (CIP) in each panel is same as lane 1 (Ark1) but treated with the phosphatase prior to loading. The band of added phosphatase is indicated by asterisk.

C. Schematic diagrams of GST-SRmut and amino acid sequence of SR protein which is used as substrate here. All of the red lines labeled threonines are mutated into alanine. And there are still 10 more threonines in the mutated SR, which are labeled with green lines.

The extensive phosphorylation of GST-SR caused the protein band to be up-shifted from 40 kDa up to about 60 kDa. Calf intestinal phosphatese(CIP) treatment of the purified GST fusion protein abolished the phosphor-threonine signal and the band-shift, indicating the anti-phosphor-threonine antibody specifically recognizes the phosphor-threonine signals. The phosphorylation was confined to the predicted Prk1p phosphorylation sites, as converting all the threonine residues in these consensus TG sites to alanine (GST-SRmut) by site-directed mutagenesis(Figure 3.2C) abolished phosphorylation by either Ark1p or Prk1p, even though numerous other threonine residues were still present. Similar experiments were also carried out with two Pan1p N-terminal long repeats (LR): LR1 and LR2 (Zeng and Cai, 1999). Ark1p phosphorylated LR1 and LR2 as efficiently as Prk1p (Figure 3.2, lower panels), and the phosphorylation of GST-LR1 and GST-LR2 caused the protein band to be up-shifted. These results showed that Ark1p is able to phosphorylate at least two of the Prk1p's native targets, Pan1p and Sla1p, *in vitro*.

3.2.3. The *in vivo* substrate preference of Prk1p and Ark1p

To test whether Ark1p contributes to the phosphorylation of Sla1p and Pan1p *in vivo*, proteins immunoprecipitated from wild type, *prk1Δ*, *ark1Δ, prk1Δ akl1Δ*, *ark1Δ prk1Δ* and *prk1Δ ark1Δ akl1Δ* cells, were examined by western blotting with anti-phospho-threonine antibody. The anti-Myc antibody was used to check the protein amount. The level of Sla1p phosphorylation from *prk1Δ, ark1Δ, ark1Δ prk1Δ,* or *prk1Δ akl1Δ* cells was similar to that of wild type cells, while no signal was detected from the triple deletion *prk1Δ ark1Δ akl1Δ* cells or

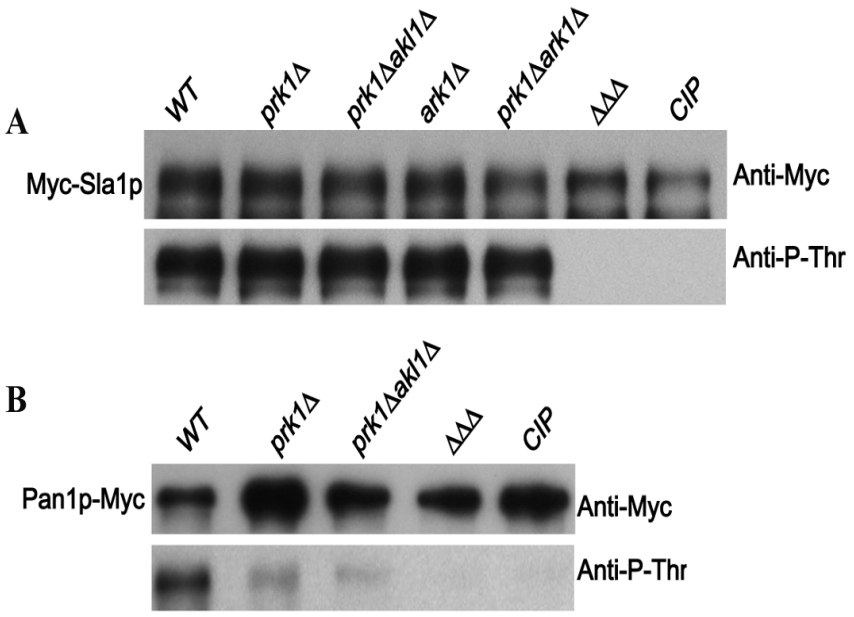

Figure 3.3. *In vivo* phosphorylation status of Sla1p and Pan1p in different kinase deletion mutants.

A. Myc-Sla1p was immunoprecipitated from cell lysate prepared from wild-type (YMC505) and five different kinase deletion strains: *prk1Δ* (YMC506), *prk1Δ akl1Δ* (YMC507), a*rk1Δ* (YMC515), *prk1pΔ ark1Δ* (YMC516) and *prk1pΔ ark1Δ akl1Δ* (YMC504/508), at 30°C. The immunoprecipitates from wild-type (YMC505) were incubated with 1 μl of CIP for 30 min at 37°C prior to loading.

B. Myc-tagged Pan1p was immunoprecipitated from cell lysate prepared from wild-type (YMC511) and three different kinase deletion strains, *prk1Δ* (YMC512), *prk1Δ akl1Δ* (YMC503), and *prk1pΔ ark1Δ akl1Δ* (YMC504), separated on SDS gels, and probed by the mouse anti-Myc antibody. The membrane was stripped and probed again with the rabbit anti-phosphothreonine antibody. The immunoprecipitates from wild-type (YMC511) were incubated with 1 μl of CIP for 30 min at 37°C prior to loading.

after phosphatase treatment (CIP), indicating that Ark1p could indeed contribute to Sla1p *in vivo* phosphorylation (Figure 3.3A). The level of Sla1p phosphorylation remained essentially unchanged as long as one of the three kinases was functional. In contrast, deletion of the *PRK1* gene alone resulted in a drastic reduction in the Pan1p phosphorylation (Figure 3.3B), suggesting that Pan1p, unlike Sla1p, is more restricted to regulation by Prk1p. The residual phosphorylation of Pan1p persists in *prk1Δ akl1Δ* mutant, but disappears in *prk1Δ ark1Δ akl1Δ*, indicating that Ark1p also contribute to Pan1p *in vivo* phosphorylation.

3.2.4. The phosphorylation motifs of Ark1

The Prk1p phosphorylation motifs have been identified as [L/I/V/M]xx[Q/N/T/S]xTG (Huang *et al.*, 2003), using the substrate derived from a fragment of Pan1 (amino acids 564-846, named as R15) that contains a single LxxQxTG motif (Figure 3.4A). As the *E.coli* co-expression assay can efficiently demonstrate Ark1p kinase activity, Ark1's potential phosphorylation motifs were examined by coexpression of Ark1 kinase domain with the various GST-R15 mutants as substrates. For convenience of description, the threonine in the LxxQxTG motif is given a position number of P0, and the residues upstream of P0 are designated as P-n (Figure 3.4A).

In a preliminary test, as shown in Fingure 3.4B, Ark1p could phosphorylate GST-R15 when they are co-expressed. The phosphor-threonine signal was not

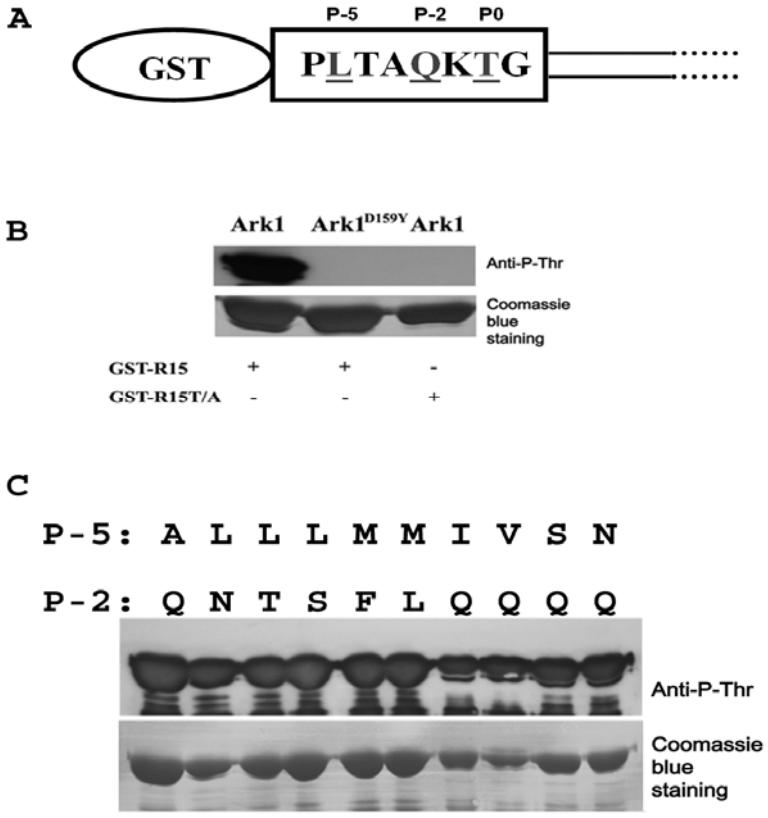

Figure 3.4 Ark1p could phosphorylate Prk1p phosphorylation motifs.

A. Schematic diagram of GST-R15.

B. Ark1p could phosphorylate LxxQxTG. The substrates GST-R15 and GST-R15T/A, indicated below the panels, were co-expressed with respective kinases, indicated above the panels, purified after 1 h induction and analyzed by SDS-PAGE and western blot. The substrate GST fusion proteins were visualized by coomassie blue staining, and the phosphorylations were detected by western blotting with anti-phosphor-threonine antibody.

C. Ark1p could phosphorylate Prk1p consensus phosphorylation motifs. The substrates GST-R15 variations, indicated above the panels, were co-expressed with Ark1p kinase domain, purified after 1 hour induction and analyzed by SDS-PAGE and western blotting.

detected when the mutant kinase Ark1^{D159Y} was used as kinase, or the GST-R15T/A (the threonine at the P0 position was mutated to alanine) was used as substrate, suggesting that Ark1p could phosphorylate GST-R15 on the threonine in the consensus LxxQxTG site. We next tested if Ark1p could phosphorylate all the other known Prk1p consensus phosphorylation sites. Besides these identified phosphorylation motifs [L/I/V/M]xx[Q/N/T/S]xTG, there are some other repeats of TG sites found in Sla1p, in which the P-5 position is [A/S/N] and P-2 position is [F/L], which may represent additional patterns of Prk1p or Ark1p phosphorylation motif. The L residue of R15-WT at P-5 was mutated into the P-5 variations in the identified Prk1p's phosphorylation motifs and some variations found in Sla1p-SR, namely A, M, I, V, and S; and the Q residue of R15-WT at P-2 was mutated into the P-2 variations in the established Prk1p's phosphorylation motifs and some variations found in Sla1p-SR, namely, N, T, S, F, and L. As shown in Figure 3.4C, Ark1p was able to phosphorylate all of these variants.

3.3 Discussion

Compared with Prk1p, Ark1p has been much less studied and its phosphorylation targets were not clear. It is, however, deemed functionally redundant to Prk1p by the fact that the mutants of either *prk1* or *ark1* have no obvious phenotypes but simultaneous loss of both proteins is disastrous for cell growth, due to the severe defects in actin organization and endocytosis. A typical case was reported by Sekiya-Kawasaki *et al.*, where inhibition of Prk1p in the *ark1* mutant led to rapid and Arp2/3-dependent accumulation of aggregated

endocytic intermediates composed of vesicles wrapped by actin filaments (Sekiya-Kawasaki *et al.*, 2003). However, the mechanism of their functional redundancy is not clear. Moreover, *PRK1* and *ARK1* have distinct genetic interactions with other endocytic proteins, indicating that some differences do exist between these two kinases. It was hypothesized that they may have different phosphorylation motifs (Smythe and Ayscough, 2003).

In this study, by a bacterial co-expression system, it was demonstrated that the kinase domains of Ark1p and Prk1p are equally efficient in phosphorylating Sla1p and Pan1p. The *in vivo* phosphorylation of Pan1p and Sla1p also depend on Ark1p in the absence of Prk1p and Akl1p. Moreover, our finding that Ark1p could phosphorylate Pan1p *in vivo* is also consistent with the report that mutations of all potential Prk1 phosphorylation sites in Pan1p resulted in actin abnormalities similarly present in *prk1Δark1Δ*, but absent from *prk1Δakl1Δ* cells (Toshima *et al.*, 2005). Both *in vitro* and *in vivo* evidence demonstrated that Pan1p and Sla1p are substrates of Ark1p and Prk1p. In addition, in the *E. coli* co-expression assay, Ark1p can phosphorylate known Prk1p phosporylation sites.

We noticed that the *in vivo* phosphorylation level of Pan1p was primarily dependent on Prk1p, as it decreased dramatically in the *prk1* mutant, whereas the Sla1p phosphorylation level remained almost unchanged with any one of the three kinases present. These *in vivo* results indicate that Pan1p and Sla1p are subjected to different modes of regulation by Ark/Prk family kinases *in vivo*, though similar phosphorylation motifs are present in both proteins.

Akl1p, the least studied member in the Ark/Prk family is also involved in the phospho-regulation of Sla1p. Sla1p phosphorylation is completely abolished

in the triple kinase deletion mutant cells, while the level of Sla1p phosphorylation remained essentially unchanged in *ark1* Δ *prk1*Δ. But its function in endocytosis and actin cytoskeleton still remained to be explored.

Chapter 4

Non-kinase domains account for distinct functions of Ark1p and Prk1p

4.1. Background

The distinct functions of Prk1p and Ark1p were first uncovered by genetic analyses. Loss of Prk1p, but not Ark1p, was found to be lethal to the *sla2Δ* mutant and caused severe actin defects in *abp1Δ* cells (Cope *et al.*, 1999). Until the present study, the molecular basis underlining the distinct genetic interactions has remained unknown.

It had been speculated that the distinct functions of Ark1p and Prk1p may be because that the two kinases recognize and phosphorylate different target sites in response to different signals (Smythe and Ayscough, 2003). But our *in vitro* and *in vivo* experimental results described in Chapter 3 showed that Ark1p could phosphorylate Sla1p and Pan1p on similar motifs as Prk1p, and moreover, the *in vivo* phosphorylation level of Pan1p was primarily dependent on Prk1p, as it decreased drastically in the *prk1*Δ mutant, suggesting that some distinct mechanisms must be at work. The most divergent part of Ark/Prk kinase family members is their non-kinase domain. The ease of genetic manipulation in yeast enabled us to evaluate the functional importance of the non-kinase domain by a domain swap approach.

4.2. Results

4.2.1. Chimeric kinses are functional

To evaluate the functional importance of the non-kinase domains of Ark1p and Prk1p, we swapped their kinase domains (1-298aa of Prk1p and 1-299aa of Ark1p) to create two chimeric kinases named Prk1n-Ark1c (with the Prk1p kinase

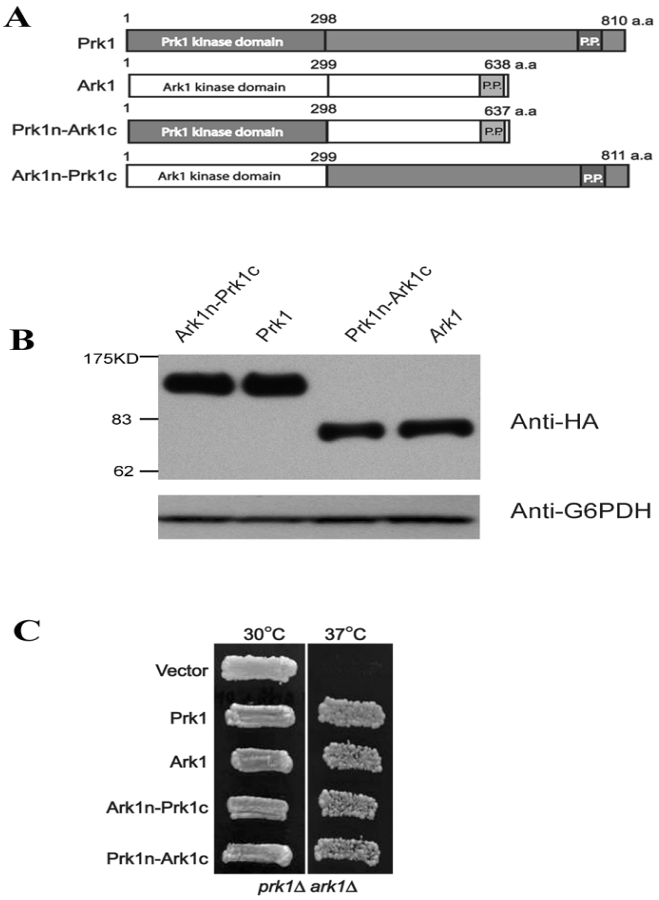

Figure 4.1 Chimeric kinases are functional.

- **A.** Schematic illustration of Prk1p, Ark1p and the chimeric kinases. Prk1n-Ark1c is made of the kinase domain of Prk1 (1 to 298 aa) and the non-kinase domain of Ark1 (300 to 638 aa), and Ark1n-Prk1c is made of the kinase domain of Ark1 (1 to 299 aa) and the non-kinase domain of Prk1 (299 to 810 aa).
- **B.** Expressions of the chimeric kinases Ark1n-Prk1c and Prk1n-Ark1C in *prk1*Δ *ark1*Δ mutant. TCA extracts from indicated cells were analyzed by western blot with anti-HA and anti-G6PDH.
- **C.** The *prk1Δ ark1Δ* mutant (YMC414) was transformed with the plasmids containing different kinase genes as indicated on the left side of the panel. The resultant strains were patched on selective medium and let grow at 30°C, and then replica-plated on a fresh plate and let grow at 37°C.

domain) and Ark1n-Prk1c (with the Ark1p kinase domain), as shown in Figure 4.1A. To check the expressions of the chimeric kinases Ark1n-Prk1c and Prk1n-Ark1C in *prk1*Δ *ark1*Δ mutant, TCA extracts from indicated cells were analyzed by western blot with anti-HA and anti-G6PDH antibodies. Both fusion genes under the *PRK1* promoter were expressed as their wild type counterparts (Figure 4.1B). After introduction into *prk1Δ ark1Δ* cells, the fusion genes were both able to rescue the mutant's temperature sensitivity at 37°C and its actin defects (Figure 4.1C), indicating that the fusion kinases are functional.

4.2.2. Non-kinase domains are responsible for distinct genetic interactions

It was found that a temperature-sensitive (ts) mutant of *PAN1*, *pan1-4*, could be suppressed by deletion of *PRK1*. However, *pan1-4* cannot be suppressed by *ARK1* deletion. We found that pan1-4 phosphorylation is dramatically decreased in *prk1*Δ mutant, but not in *ark1*Δ (Figure4.2B), which is consistent with the finding described in Chapter 3 that Pan1p phosphorylation primarily depends on Prk1p but not Ark1p.

We next tested the function of the chimeric kinases on Pan1p, by transforming the kinases into the *pan1-4 prk1Δ* cells. Strikingly, after the chimeric kinases were introduced into *pan1-4 prk1Δ* cells, it was Ark1n-Prk1c that mimicked the activity of Prk1p to reconstitute the temperature sensitivity in the mutant (Figure 4.2A).

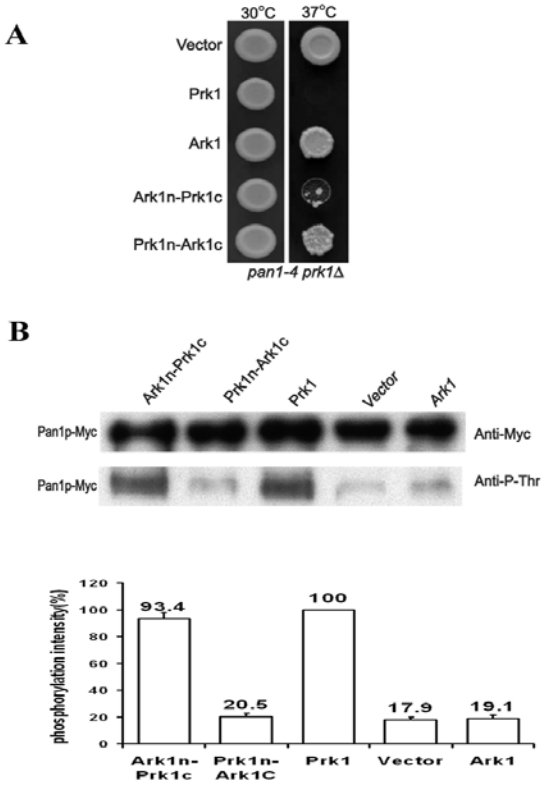

Figure 4.2 Non-kinase domains are responsible for the distinct functions of ark1/Prk1p on Pan1p

- **A.** The *pan1-4 prk1Δ* mutant (YMC413) was transformed with the plasmids as indicated and the cells were grown to log phase and spotted onto a selective plate and incubated at 30 (left) or 37°C (right). Photographs were taken after each plate was incubated for 2 days.
- **B.** The *prk1Δ ark1Δ* mutant containing Myc-Pan1p (YMC509) was transformed with the different kinase constructs. Myc-Pan1p was immunoprecipitated from cell lysates prepared from strains indicated above the panel, gel separated and probed sequentially by mouse anti-Myc and rabbit anti-phosphothreonine antibodies. The phosphorylation level of Pan1-Myc in each sample was measured by densitometer and normalized against its protein amount. The relative phosphorylation intensities were calculated and presented as bar graphs shown below.

As Pan1p phosphorylation in *vivo* mainly depends on Prk1p (Chapter3), Pan1p phosphorylation status in the various chimeric kinases background was examined as well. The immunoprecipitated Pan1p was examined by western blot with an anti-Myc antibody to verify the protein amount and the phosphorylation status was checked by western blot with anti-phospho-threonine antibody. The phosphorylation level of Pan1-Myc in each sample was measured by densitometer and normalized against its protein amount. The relative phosphorylation intensities were calculated and presented as bar graphs. Consistently, the level of Pan1p phosphorylation was similarly high in the cells expressing Prk1p and Ark1n-Prk1cp, and almost equally low in Ark1p and Prk1n-Ark1cp containing cells (Figure 4.2B). Taken together, these results indicate that the non-kinase domain is responsible for the distinct *in vivo* functions of Prk1p and Ark1p.

4.2.3. The function of Ark1p, but not Prk1p, depends on the C-terminal polyproline motif

One important feature of the non-kinase domains of Ark1p and Prk1p is their C-terminal poly-proline motif. The localization of Ark1p and Prk1p to the cortical actin patches has been shown to be mediated by an interaction between these C-terminal poly-P motifs and the SH3(Src homology 3) domain of Abp1p (Cope *et al.*, 1999; Fazi *et al.*, 2002). However, deletion of *ABP1* does not produce a similar phenotype as observed in *prk1Δ ark1Δ*. In addition, unlike Ark1p, whose cortical association was completely eliminated in the *abp1*Δ mutant, the cortical localization of some Prk1p proteins has been observed in the *abp1*Δ mutant (Cope

et al., 1999; Fazi *et al.*, 2002). Therefore, we hypothesized that Prk1p may have additional ways to be localized cortically. It is possible that the Prk1 poly-proline motif may be able to bind to other SH3 motif containing actin patch proteins.

To reassess the functions of their polyproline motifs, we created *prk1* and *ark1* mutants lacking only the polyproline motifs and transformed them into *prk1Δ ark1Δ* cells. The expression levels of Prk1pΔPP and Ark1pΔPP were confirmed by western blotting to be similar to their wild type counterparts (Figure 4.3D). As shown in Figure 4.3A, Prk1pΔPP could complement the temperature sensitivity of *prk1Δ ark1Δ* at 37°C, while Ark1pΔPP could not. Consistent with this, Prk1pΔPP-GFP was still able to localize to the cortical patches, while Ark1pΔPP-GFP was diffused in the cell (Figure 4.3 B). Moreover, Prk1pΔPP also rescued the actin defects in the *prk1Δ ark1Δ* cells to an extent indistinguishable from the wild type, whereas considerable actin aggregates were still visible in the cells expressing Ark1pΔPP, although in smaller sizes than those in *prk1Δ ark1Δ* cells (Figure 4.3C). These results suggest that Prk1p, but not Ark1p, could function independently of the polyproline motif and the patch localization of Prk1p may depend on other region in its non-kinase domain. This suggestion is also consistent with an earlier observation that the *prk1Δ abp1Δ* mutant acquired a similar actin defect as in the *prk1Δ ark1Δ* mutant whereas the *ark1Δ abp1Δ* mutant did not (Cope *et al.*, 1999).

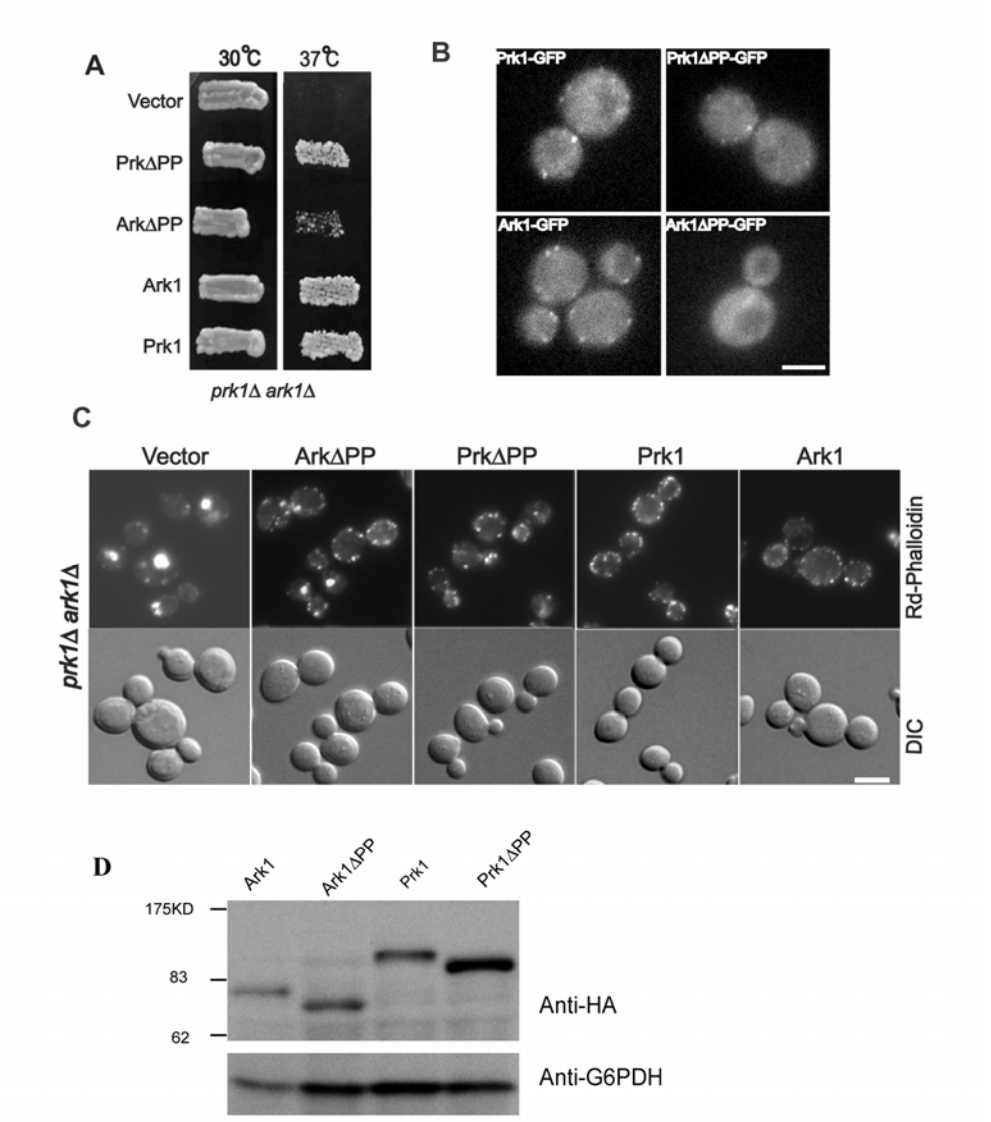

Figure 4.3 The function of Ark1p, but not Prk1p, depends on the C-terminal polyproline motif

A. The *prk1Δ ark1Δ* mutant (YMC414) was transformed with single-copy plasmid carrying *PRK1*, *ARK1*, *PRK1ΔPP* and *ARK1ΔPP* (with deletions in the polyproline stretch). The resultant strains were patched on selective medium at 30°C (left), and replica-plated on a fresh plate and incubated at 37°C (right). Photographs were taken after each plate was incubated for 2 days.

B. Prk1p, but not Ark1p, can localize to cortical patches without the C-terminal poly-P motif. Plasmids carrying GFP tagged

Prk1p, Ark1p, Prk1ΔPP and Ark1ΔPP, each under their native promoters, were transformed into *prk1Δ* (YMC410) or *ark1Δ* (YMC409), and the transformants were examined under fluorescent microscope.

C. Rhodamine-phalloidin staining of actin filaments in the cells described above. Scale bars, 5 μm.

D. Expression of Prk1p, Ark1p, Prk1ΔPP and Ark1ΔPP proteins in the transformed *prk1Δ ark1Δ* cells. TCA precipitates from the extracts of cells shown in Figure 3A were analyzed by immunoblotting with anti-HA antibody and anti-G6PDH.

4.3. Discussion

4.3.1. Non-kinase domain is responsible for distinct function of Ark1p and Prk1p

In Chapter 3, we have demonstrated that Ark1p's kinase activity is comparable with Prk1p in *E. coli* co-expression assay. Moreover, Prk1p and Ark1p are divergent outside their highly homologous kinase domains. It is reasonable to speculate that the distinct functions of Ark1p and Prk1p may be mediated by their divergent C-terminal regions. This was proved to be true by the domain swap experiments. It is rather conspicuous that the Pan1p phosphorylation was recovered nearly to the wild-type level by the kinase domain of Ark1p fused to the non-kinase domain of Prk1p, while the Prk1p kinase domain became incompetent to perform what used to be its native task after it equipped with the non-kinase domain of Ark1p. Clearly, the non-kinase domains are crucial for the differential activities of Prk1p and Ark1p, at least as shown by the phosphorylation of Pan1p.

4.3.2. Prk1p has poly-proline independent anchor

The poly proline motif is the only known element in the non kinase region that is important for the function of the kinases. It has been shown to be responsible for the patch localization of Ark1p and Prk1p through the interaction with Abp1p SH3 domain (Fazi *et al.*, 2002). By evaluation of the contributions of polyproline motif, we found that the function of Ark1p essentially depends on the polyproline motif, whereas Prk1p is still functional in the absence of its poly-P motif. Prk1pΔPP is not only able to rescue the temperature-sensitivity and actin defects of a*rk1Δ prk1Δ*, but also able to reconstitute the temperature-sensitivity in the *pan1-4 prk1Δ* mutant (Figure 5.3). In fact, Prk1pΔPP-GFP was still able to localize to the cortical patches, suggesting that Poly-P motif is not the sole determinant for the actin patch localization of Prk1p. The existence of poly-P independent recruiter could also explain why Prk1p can still localize to actin patch in the absence of Abp1p. We hypothesize that the functions of Ark1p and Prk1p kinases are regulated by distinct anchors which determine their spatial and temporal localizations in the endocytic machinery.

Chapter 5

Identification of Arp2p as a new anchor for Prk1p

5.1. Background

Phosphorylation is one of the most common regulatory methods present in all organisms. As unregulated phosphorylation would be harmful to cells, it is vital to keep the activity of these kinases under proper control. Controlled sub-cellular positioning is an important way to ensure the protein kinase to be positioned at the right place and right time to perform its respective function.

The studies of Prk1ΔPP and Ark1ΔPP in Chapter 4 have established that *in vivo* functions of Ark1p and Prk1p are closely connected to the cortical patch localization. The results also indicate that Prk1p has a poly proline independent anchor, which prompted us to search for proteins that interact with the C-terminal region of Prk1p but independent of polyP. Identification of Prk1p's Poly-P independent anchor will shed light on the underlying mechanism of the redundant and distinct functions of Ark1p and Prk1p, and the regulation of the kinases during endocytic vesicle internalization and pinching off.

5.2. Results

5.2.1. Identification of Arp2p as a binding protein for Prk1p

The yeast two-hybrid system was used to test interactions of Prk1pΔPP with a number of known actin patch-associated proteins including Pan1p, Sla1p, End3p, Scd5p, Sac6p, Cap1p, Cap2p, Arp2p and Arp3p. Among them, Arp2p, the core component of Arp2/3 complex, was found capable of binding to Prk1pΔPP but not to Ark1pΔPP (Figure 5.1A). Using various deletion constructs of Prk1p, the region necessary for interacting with Arp2p was mapped to a 21-amino-acid region (299-319 aa.) adjacent to the kinase domain.

To determine whether the interaction between Prk1p and Arp2p is direct, the binding between His-tagged Arp2p and GST-Prk1$_{1-319}$ was investigated. Equal amounts of bead-immobilized GST-Prk1$_{1-319}$ and GST-Prk1$_{1-298}$ (kinase domain only) were mixed with equal amount of purified His-Arp2, respectively. After washing, the bound proteins were analyzed by western blot with anti-GST and anti-His antibodies. As shown in Figure 5.1B, His-Arp2 could be precipitated by GST-Prk1$_{1-319}$ but not by GST-Prk1$_{1-298}$, indicating that the 21-amino-acid segment between 298 and 319 is required for the direct binding of Prk1p to Arp2p.

The interaction between Prk1p and Arp2p was further confirmed by co-immunoprecipitation. The *PRK1* gene without the C-terminal poly proline region, *PRK1ΔPP*, was tagged with the Myc-epitope and placed under the *GAL1* promoter to enhance its expression. After galactose induction for 2 h, cell lysates were prepared and Myc-Prk1p was precipitated. As shown in Figure 5.1C, HA-Arp2 could be co-immunoprecipited by the anti-Myc antibody. The co-immunoprecipitation was abolished if the 21 a.a. region of Prk1p was replaced by the corresponding region from Ark1p (Prk1$_{AR}$ΔPP) (Figure5.1C).

5.2.2. Interaction with Arp2p is important for Prk1p's patch localization

To test whether the 21 a.a. region was required for Prk1p to achieve the cortical localization, GFP fusion proteins of wild type Prk1p, Prk1$_{1-319}$, Prk1$_{1-298}$, Prk1$_{AR}$, and Prk1$_{AR}$ΔPP were placed under the control of *GAL1* promoter and transformed into wild type cells. The cortical GFP signals were observed only in the cells expressing Prk1-GFP, Prk1$_{1-319}$-GFP, and Prk1$_{AR}$-GFP. On the other hand, the GFP signals of Prk1$_{1-298}$-GFP and Prk1$_{AR}$ΔPP-GFP were diffused in the

A Two-hybrid interaction between Prk1p and Arp2p

Bait	Prey: pGADT7 (vector)	Prey: Arp2p
pGBKT7(vector)	<0.5	<0.5
$Prk1^{D158Y}$p(1-810 a.a.)	<0.5	147±14.5
$Prk1^{D158Y}$p(1-747 a.a.)	<0.5	153±17.3
$Prk1^{D158Y}$p(1-319 a.a.)	<0.5	132±12.1
$Prk1^{D158Y}$p(1-298 a.a.)	<0.5	<0.5
$Ark1^{D159Y}$p (1-638 a.a.)	<0.5	<0.5

(units of β-galactosidase activity)

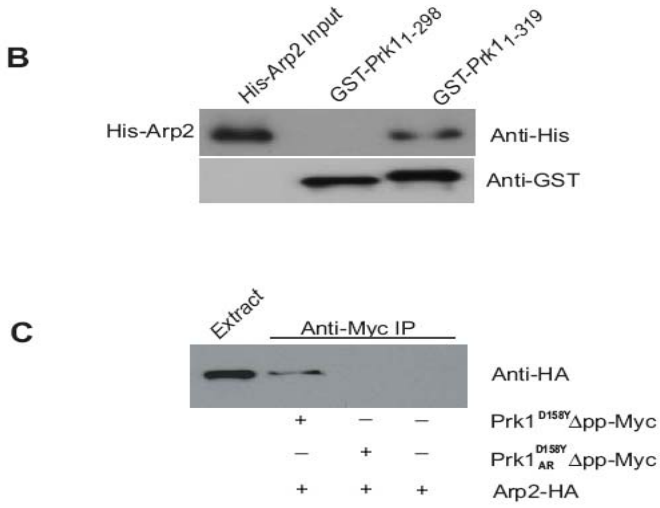

Figure 5.1. Identification of Arp2p as a new adapter protein for Prk1p.

A. Two-hybrid interaction between Prk1p and Arp2p.

B. *In vitro* binding of Arp2p with Prk1p. GST fusion proteins of $Prk1_{1\text{-}319}$ and $Prk1_{1\text{-}298}$ were immobilized on glutathione-agarose beads and incubated with His-Arp2. Bound proteins were analyzed by Western blotting with the anti–His antibody and the GST fusion proteins were detected by the anti-GST antibody.

C. Co-immunoprecipitation of Prk1p and Arp2p. Yeast extracts in equal amounts prepared from YMC510 (*arp2::* Arp2-HA) and YMC510 containing pGAL-$PRK1^{D158Y}$ΔPP-Myc or pGAL-$Prk1^{D158Y}{}_{AR}$ΔPP-Myc were subjected to anti-Myc immunoprecipitation. The bound proteins were analyzed by immunoblotting with anti-HA antibody. Extracts used are shown below the gel. The extract lane is the extracts from the pGAL- $PRK1^{D158Y}{}_{AR}$ΔPP-Myc containing strain.

cytoplasm (Figure 5.2). This result indicates that either the Arp2p-interacting region or the Abp1p-interacting region is sufficient for Prk1p to be localized to cortical patches. Moreover, we also noted that more than 90% of the Prk1-GFP and $Prk1_{1-319}$-GFP patches colocalized with the actin patches, which is a common feature of actin module proteins including Abp1p, Arp2/3 complex, Cap1/2p (Kaksonen et al., 2005).

5.2.3. Prk1p patch localization closely correlates to Prk1p's function

To evaluate the functional significance of the Arp2p-Prk1p interaction, wild type Prk1p, $Prk1_{1-319}$, $Prk1_{1-298}$ and $Prk1_{AR}$ (with the polyproline region), was transformed into *prk1Δ ark1Δ* cells. All the mutant kinase proteins were stable and expressed well (Figure5.3A). The resultant strains were tested for growth at 37°C. Wild type Prk1p, $Prk1_{1-319}$ and $Prk1_{AR}$ could rescue the temperature sensitivity of *prk1Δ ark1Δ* at 37°C, whereas the kinase domain alone ($Prk1_{1-298}$) failed to do the same (Figure 5.3B, left panel). We also examined the actin structures of these cells by Rhodamin Phalloidin (Rd-Phallo idin) staining. Consistent with above temperature sensitivity results, wild type Prk1p, $Prk1_{1-319}$ and $Prk1_{AR}$ could rescue the actin defect, while kinase domain alone ($Prk1_{1-298}$) and $Prk1_{AR}\Delta PP$ failed to do the same (Figure 5.3C, lower panel). As endocytosis depends on normal actin structures in yeast, the endocytic functions of these kinase mutant cells were also investigated. Indeed, wild type Prk1p, $Prk1_{1-319}$ and $Prk1_{AR}$ could rescue the defect in Lucifer Yellow uptake of the *prk1Δ ark1Δ* cells, but $Prk1_{1-298}$ and $Prk1_{AR}\Delta PP$ could not (Figure 5.3C upper

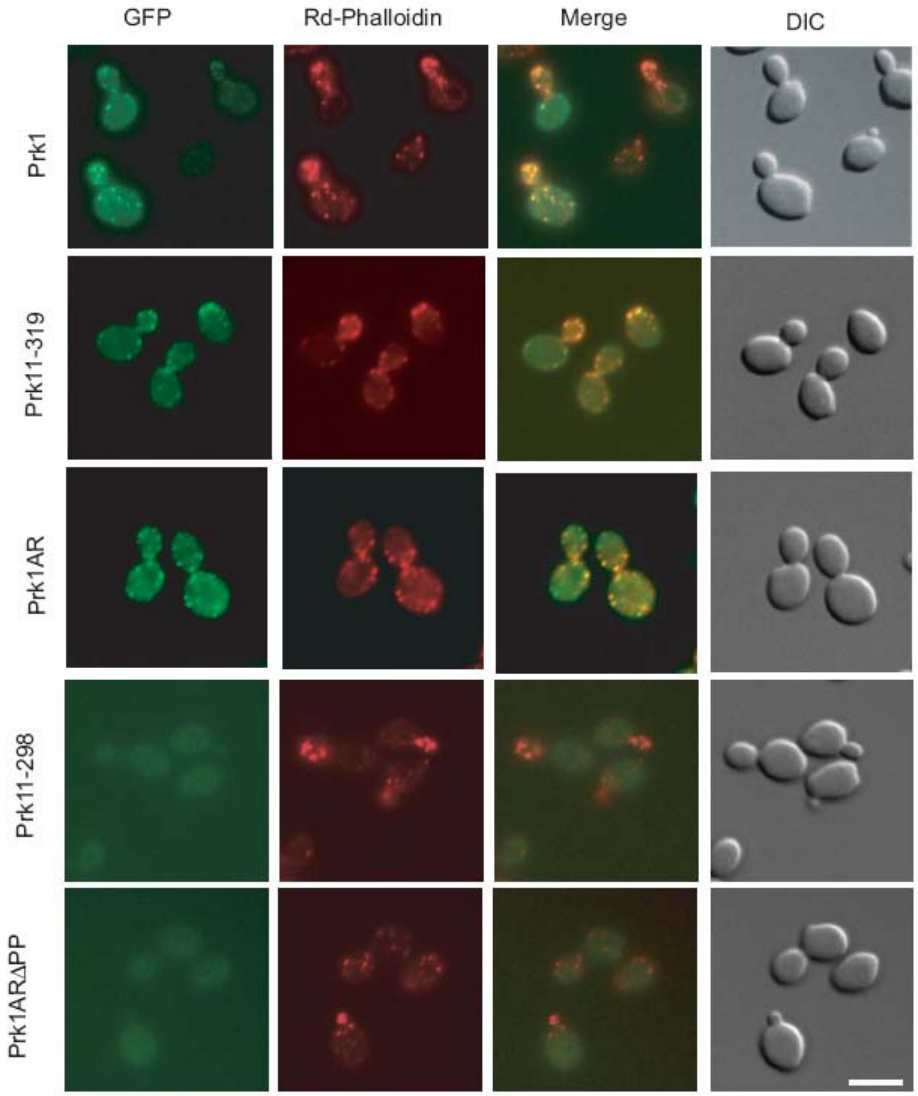

Figure 5.2. The Arp2p binding region of Prk1p is required for its cortical localization.

Wild type cells (W303-1A) were transformed with plasmids carrying pGAL-PRK1^{D158Y}-GFP, pGAL-PRK1$^{D158Y}{}_{1\text{-}319}$-GFP, pGAL-PRK1$^{D158Y}{}_{1\text{-}298}$-GFP, pGAL-PRK1$^{D158Y}{}_{AR}$-GFP and pGAL-PRK1$^{D158Y}{}_{AR}$ΔPP-GFP. After 1 hour galactose induction, cells were fixed and stained with rhodamine (Rd)-phalloidin. Since over-expression of Prk1p could disturb actin cytoskeleton, an inactive kinase (D158Y) was used in this experiment.

panel). These results suggest that as long as the localization to the cortical patches is achieved, either by the interaction with Arp2p (shown by $Prk1_{319}$) or with Abp1p (shown by $Prk1_{AR}$), Prk1p will be able to perform the essential functions. But, when the C terminal region is deleted, the kinase domain alone ($Prk1_{298}$) cannot perform the kinase function, though the kinase domain alone still could phosphorylate substrates in vitro (Chapter3).

5.2.4 Arp2p binding is important for regulation of Pan1p by Prk1p

As we discussed in the Chapter 4, the non-kinase domains are critical for the differential activities of Prk1p and Ark1p, at least as shown in the phosphorylation of Pan1p. With the identification Arp2p as Prk1p's new anchor protein, we are now able to answer the question of whether interaction with Arp2p differentiates Prk1p from Ark1p. Wild type Prk1p, $Prk1_{1\text{-}319}$, $Prk1_{1\text{-}298}$ and $Prk1_{AR}$ (with the polyproline region), was transformed into *pan1-4 prk1Δ* cells. All the mutant kinase proteins were stable and expressed well (Figure5.3A). The resultant strains were tested for growth at 37°C. Interestingly, only wild type Prk1p and $Prk1_{1\text{-}319}$ could restore the temperature sensitivity to *pan1-4 prk1Δ* cells at 37°C, whereas $Prk1_{AR}$, despite its ability to localize to the cortical patches and to rescue the double kinase deletion mutant, failed to do so (Figure 5.4A). It indicates that the interaction with Arp2p, rather than Abp1, enables Prk1p to perform its specific functions.

As the *in vivo* phosphorylation of Pan1p largely depends on Prk1p, we were interested in finding out whether the Prk1p-dependent Pan1p *in vivo* phosphorylation is mediated by Arp2p, the phosphorylation status of Pan1p was

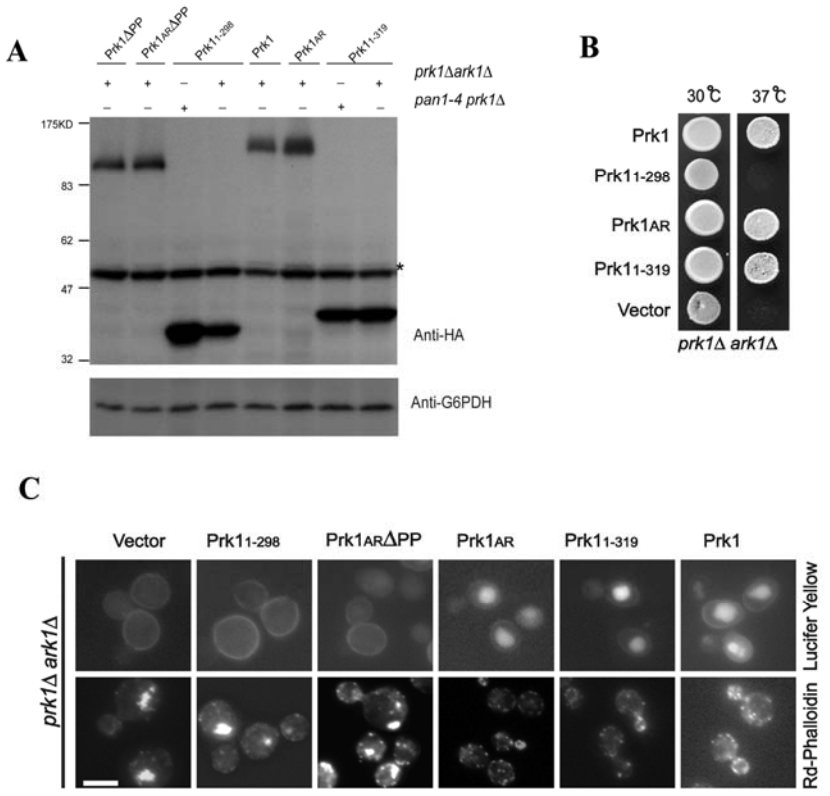

Figure 5.3 Prk1p patch localization closely correlates to its function

A. Expression of various Prk1 mutant proteins. Prk1AR, $Prk1_{AR}\Delta PP$, $Prk1_{1\text{-}298}$, $Prk1_{1\text{-}319}$, Prk1ΔPP, and Prk1, fused with the HA tag at their C terminus and placed under the native *PRK1* promoter, were transformed into the *prk1Δ ark1Δ* or *pan1-4 prk1Δ* mutants. TCA extracts from indicated cells were analyzed by immunoblotting with anti-HA and anti-G6PDH. The non-specific band is indicated by asterisk.
B. The *prk1Δ ark1Δ* (YMC414) strains were transformed with the constructs as indicated. The resultant cells were grown to log phase and spotted on selective medium and incubated at 30°C (left), and 37°C (right). Photographs were taken after cells were grown for 2 days.
C. Endocytosis and actin structures of different *prk1 mutants. The YMC414 (prk1Δ ark1Δ*) cells carrying different constructs as indicated were subjected to staining for actin filaments and the Lucifer yellow uptake assay. Scale bar, 5μm.

analyzed in the *prk1Δ ark1Δ* mutant carrying Prk1p, $Prk1_{1-319}$, $Prk1_{1-298}$ or $Prk1_{AR}$. Indeed, $Prk1p_{1-319}$ restored Pan1p phosphorylation close to the wild type level, whereas $Prk1_{1-298}$ had no effect (Figure 5.4B). $Prk1_{AR}$ was able to increase the Pan1p phosphorylation level only slightly, approximately to the residual Pan1p phosphorylation level remained in the *prk1Δ* mutant (about 20% of the wild type level).

Next we tested whether the 21 a.a region is sufficient to provide Prk1p specific function. We created another chimeric kinase, $Ark1_{PR}$, carrying the 21 a.a sequence at the corresponding region of Ark1p. HA tagged $Ark1_{PR}$ was transformed into *prk1Δ ark1Δ* cells. $Ark1_{PR}$-HA is stable and expressed as well as wild type Ark1p (Figure 5.4 C). The resultant strains were tested for growth at 37°C. $Ark1_{PR}$ could rescue the temperature sensitivity of *prk1Δ ark1Δ* at 37°C, indicating that $Ark1_{PR}$ is functional (Figure 5.4 D left panel). It was also introduced into the *pan1-4 prk1Δ*, and strikingly, $Ark1_{PR}$, similar to Prk1p and Prk1ΔPP, restored the temperature sensitivity to *pan1-4 prk1Δ* cells at 37°C (Figure 5.4D, right panel), suggesting that the Arp2p binding region renders Ark1p the ability to perform the Prk1p specific function.

5.2.5 The reconstitution of *pan1-4prk1*Δ temperature sensitivity by various kinases is closely correlated with Pan1-4p phosphorylation status in these mutants

Throughout our study, the temperature sensitivity of the *pan1-4* mutant was used to assay the function of Prk1p, Ark1p and their derivatives. However, it

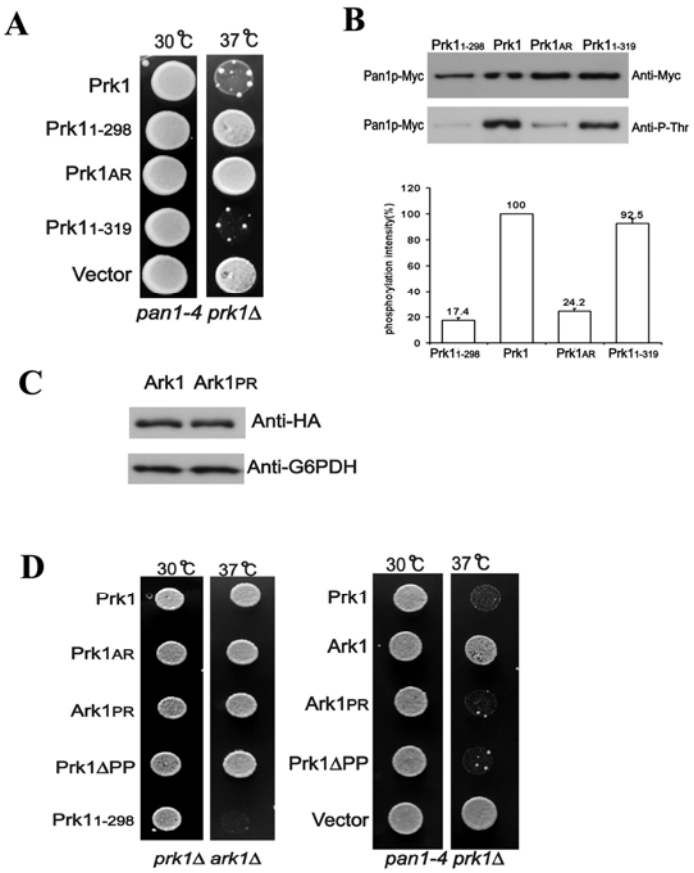

Figure 5.4 Arp2p binding is important for regulation of Pan1p by Prk1p

A. *pan1-4 prk1Δ* (YMC413) strains were transformed with the constructs as indicated. The resultant cells were grown to log phase and spotted on selective medium and incubated at 30°C (left), and 37°C (right). Photographs were taken after cells were grown for 2 days.

B. Phosphorylation status of Pan1p in different *prk1* mutants. The *prk1Δ ark1Δ* mutant containing Myc-Pan1p (YMC509) was transformed with the different kinase constructs as indicated. Myc-Pan1p was immunoprecipitated, SDS gel separated and probed sequentially by anti-Myc and anti-phosphothreonine antibodies (upper). The phosphorylation level of Pan1-Myc in each sample was normalized against its protein amount. The relative phosphorylation intensities were calculated and presented as bar graphs (lower).

C. Expression of Ark1p and $Ark1_{PR}p$ in *prk1Δ ark1Δ* mutant. TCA extracts from indicated cells were analyzed by immunoblotting with anti-HA and anti-G6PDH.

D. **Left:** *prk1Δ ark1Δ* mutant (YMC414) was transformed with plasmids containing different kinase genes as indicated. The resultant strains were grown to log phase and spotted onto a selective plate and incubated at 30 (left) or 37°C (right). **Right:** *pan1-4 prk1Δ* (YMC413) was transformed with plasmids containing different kinase genes as indicated. The resultant strains were grown to log phase and spotted onto a selective plate and incubated at 30 (left) or 37°C (right). Photographs were taken after each plate was incubated for 2 days.

remained to be determined if Pan1-4p in vivo phosphorylation status is indeed correlated with the growth phenotype. So, we next examined the *in vivo* phosphorylation status of Pan1-4p in *pan1-4 prk1*Δ strains carrying the various forms of kinases. Myc-tagged Pan1-4p was expressed under its endogenous promoter as the sole copy of Pan1p in otherwise wild type cells and *prk1*Δ mutant cells. The cells were grown at 25^oC and 37^oC. Pan1-4p proteins were immunoprecipitated by anti-Myc conjugated beads and examined by immunoblotting with an anti-Myc antibody to check the protein amount and with anti-phosphor-threonine antibody to test the phosphorylation status. The pan1-4 mutant protein (Pan1-4p) exhibited a high steady-state level of phosphorylation at 37^oC in the presence of wild type Prk1p (Figure 5.5 A). Similarly high level of phosphorylation was maintained by the kinase variants, Ark1n-Prk1c and $Ark1_{PR}$ which possessed the Arp2p-binding capacity, but not by Ark1, Prk1n-Ark1c, and $Prk1_{AR}$ that did not (Figure 5.5 B).

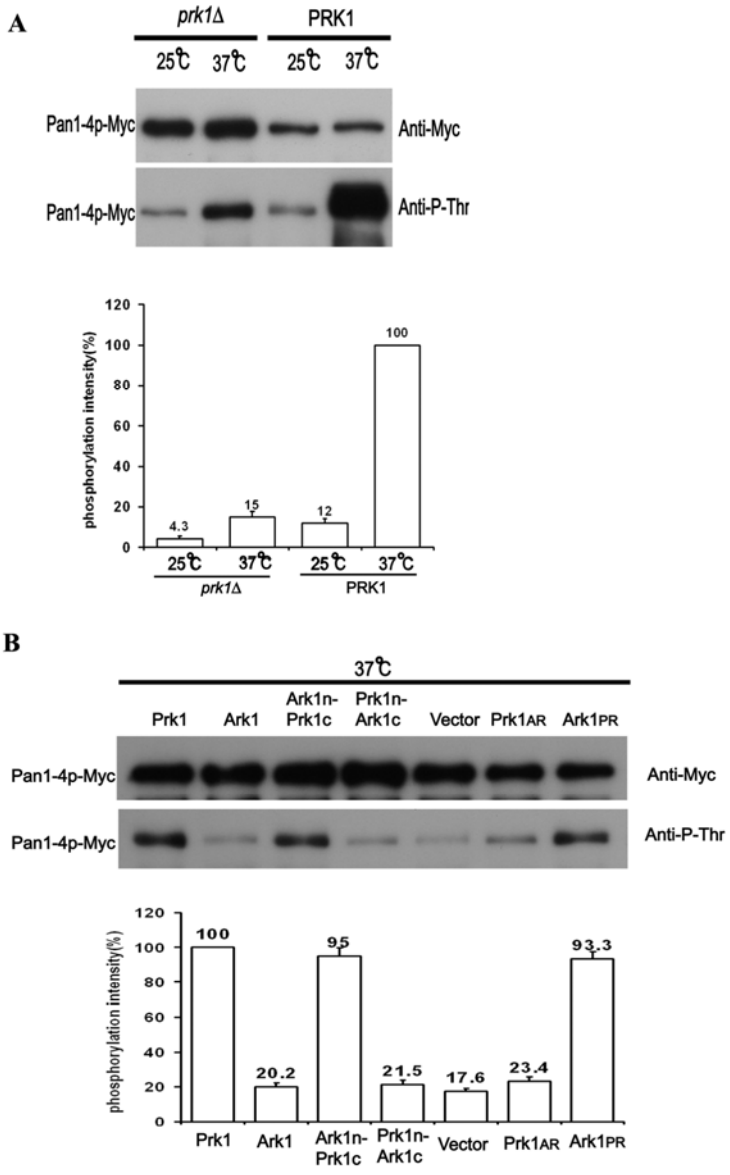

Figure 5.5 Arp2p binding is important for phosphorylation of Pan1-4p by Prk1p

A. Endogenously expressed Pan1-4p-Myc was immunoprecipitated from YMC514 (*prk1Δ*) and YMC513 (*PRK1*) cells at either 25°C (lanes 1, 3) or 37°C (lanes 2, 4) for 3 h, SDS gel separated and sequentially immunoblotted with anti-PThr and anti-Myc antibodies. The phosphorylation level of Pan1-4p-Myc in each sample was measured by densitometer and normalized against its protein amount. The relative phosphorylation intensities were calculated and presented as bar graphs.

B. Phosphorylation status of Pan1-4p in different *prk1* mutants. Endogenously expressed Pan1-4p-Myc was immunoprecipitated at 37°C from YMC 514(*prk1Δ*) cells containing pPrk1-HA-316, pArk1-HA-316, pArk1n-Prk1c-HA-316, pPrk1n-Ark1c-HA-316, pRS316, pPrk1$_{AR}$HA-316, pArk1$_{PR}$-HA-316. The relative phosphorylation intensities were calculated and presented as bar graphs.

In summary, Arp2p, the core component of Arp2/3 complex, was found capable of binding to Prk1pΔPP but not to Ark1pΔPP by using the yeast two-hybrid system. The Arp2p-Prk1p interaction appears to be direct as shown in the in-vitro binding assay. Moreover, the 21a.a. binding region of Prk1p is required for the in-vitro binding. Subsequent genetic and biochemistry studies indicate that the region is not only important for Prk1p patch localization, but also important for Prk1p's distinct function on Pan1p.

5.3. Discussion

5.3.1. Arp2p as a new anchor protein of Prk1p

Ark1p and Prk1p are known as negative regulators of actin and endocytic coat complex during the endocytic internalization (Zeng *et al.*, 2001; Sekiya-Kawasaki *et al.*, 2003). Although several Prk1p substrates have been identified, how Ark1p and Prk1p are regulated to disassemble the endocytic coat is still unknown. Conceivably, the assembly and disassembly of coat complex and actin polymerization must be tightly coordinated. Early arrival of Prk1p and Ark1p may cause inefficient or abortive coat assembly; late arrival of these kinases may result in delayed coat disassembly and excessive actin assembly. Abp1p is a known adapter involved in their recruitment, through the specific binding occurs between

Abp1-SH3 and the poly proline motif in the kinases' non-kinase domain (Cope *et al.*, 1999; Fazi *et al.*, 2002). However, as an *abp1*Δ mutant does not show drastic defects as in *ark1*Δ *prk1*Δ, and Prk1p still can localize to endocytic sites in *abp1*Δ, other anchor(s) is proposed to be responsible for recruiting Prk1p to the endocytic sites. In this study, we found that Prk1p without Poly P still can localize to actin patches and rescue the temperature sensitivity phenotype, as well as actin and endocytic defects of *ark1*Δ *prk1*Δ. Through a small scale directed yeast two-hybrid screen, we identified Arp2p, a key component of Arp2/3 complex, as a new anchor responsible for Prk1p's patch localization and function. The live image study showed that Arp2/3 complex arrives at cortical endocytic site, together with Abp1p, Actin, Sac6p (yeast fimbrin), and Cap1/2p, which are classified into the actin module (Kaksonen *et al.*, 2005). The arrival of Arp2/3 complex and Abp1p on the patch marks the turning point from coat assembly to actin polymerization and membrane invagination. On the other hand, almost all of the known Prk1p substrates, such as Pan1p, Sla1p and Scd5p (may also include Ent1/2p and YAP1801/1802p), are shown to assemble to the endocytic sites earlier than actin module, hence they are not likely to be phosphorylated by Ark1/Prk1 until the endocytic coat matures. Therefore, using Arp2p and Abp1p as anchors is an ideal way to timely coordinate the coat assembly and disassembly in a timely way during endocytic internalization.

The discovery of Arp2p as Prk1p's anchor protein is not the first case of the Arp2/3 complex functioning beyond its actin assembly activity. In a recent study, Arp2/3 complex is also found to interact with exocyst component Exo70 to

coordinate cytoskeleton and membrane traffic during cell migration (Zuo *et al.*, 2006).

5.3.2. Arp2p and Abp1p recruited Prk1p have different effect on Pan1p

Compared with Abp1p, Arp2p recruits a much less amount of Prk1p, as Prk1-GFP signal reduced considerably in an *abp1*Δ mutant. Nevertheless, Arp2p-mediated Prk1p appears to be more important for phosphor-regulation of Pan1p than Abp1p. Because Pan1p is known to interact with many endocytic proteins including End3p, Sla1p, Sla2p, Ent1/2p, Yap1801/2p, and Scd5p, it is conceivable that Pan1p may exist in different complexes which locate to different regions in the endocytic coat complex. Moreover, all the known Arp2/3 activators, such as Bee1p/Las17p, Myo3/5p, and Pan1p, not only recruit Arp2/3 complex, but also have interactions with numerous endocytic proteins. Thus, it is possible that Arp2p mediated Prk1p may be directed to a pool of Pan1p complex which is not accessible by Abp1p mediated Prk1p.

5.3.3. Implications of Arp2p-recruited Prk1p on Pan1p function

Pan1p is a key component of the cellular machinery responsible for actin organization and endocytosis. It not only acts as a scaffold for assembly of the endocytic complex by interacting with a number of endocytic proteins, but also acts as a linker to connect the vesicle and actin filament meshworks, by interaction with actin filaments and stimulating Arp2/3 complex to activate actin filaments nucleation at the endocytic site**.** Toshima *et al*., found that Prk1p inhibited the ability of Pan1p to bind to actin filaments and to activate the Arp2/3

complex, supporting that phosphorylation of Pan1p by Prk1p is an important mode of regulation during endocytosis Prk1p (Toshima *et al.*, 2005). Though, it is not clear yet which specific step does Pan1p exactly function in, it is likely that Pan1p-promoted actin assembly at the endocytic sites may only need to be very transient, and such a brief burst of actin polymerization may be sufficient for that particular step of event, to induce membrane invagination, for example.

The discovery of Arp2p as a new Prk1p anchor protein indicates that an auto-limiting mechanism may be at work in this process. As Prk1p, an inhibitor of the actin nucleation by Pan1p, is recruited together with Arp2p, a component of the actin nucleation factor Arp2/3 complex, to the endocytic sites after the assembly of endocytic coat, it appears that the actin assembly engine is equipped with a brake when it starts working.

In conclusion, we characterized the kinase activity of Ark1p and identified Pan1p and Sla1p as Ark1's substrates, which explained the functional redundancy of Prk1p and Ark1p in actin patch and endocytosis regulation. We also found that although Pan1p can be phosphorylated by both kinases, Prk1p appears to play a major role. The functional difference between Prk1p and Ark1p is due to their non-kinase domains through domain-swap analysis. Next, Arp2p, a component of Arp2/3 complex, was identified as a new anchor for Prk1p, but not for Ark1p. Genetic and biochemical data also supported that the interaction between Prk1p and Arp2p decides the distinctive function of Prk1p. Together with Abp1p, a known anchor for Prk1p and Ark1p, this finding suggests that Ark1p and Prk1p, two negative regulators of endocytic coat, are recruited simultaneously with actin

assembly, providing an important insight on how cells coordinate the endocytic coat formation, actin assembly and disassembly.

Reference

Adams,A.E., Pringle,J.R. (1984). Relationship of actin and tubulin distribution to bud growth in wild-type and morphogenetic-mutant Saccharomyces cerevisiae. J Cell Biol *98*, 934-945.

Amberg,D.C. (1998). Three-dimensional imaging of the yeast actin cytoskeleton through the budding cell cycle. Mol Biol Cell *9*, 3259-3262.

Ayscough,K.R. (2000). Endocytosis and the development of cell polarity in yeast require a dynamic F-actin cytoskeleton. Curr Biol *10*, 1587-1590.

Ayscough,K.R., Stryker,J., Pokala,N., Sanders,M., Crews,P., Drubin,D.G. (1997). High rates of actin filament turnover in budding yeast and roles for actin in establishment and maintenance of cell polarity revealed using the actin inhibitor latrunculin-A. J Cell Biol *137*, 399-416.

Barany,M., Barron,J.T., Gu,L., Barany,K. (2001). Exchange of the actin-bound nucleotide in intact arterial smooth muscle. J Biol Chem *276*, 48398-48403.

Bi,E., Maddox,P., Lew,D.J., Salmon,E.D., McMillan,J.N., Yeh,E., Pringle,J.R. (1998). Involvement of an actomyosin contractile ring in Saccharomyces cerevisiae cytokinesis. J Cell Biol *142*, 1301-1312.

Boucrot,E., Saffarian,S., Massol,R., Kirchhausen,T., Ehrlich,M. (2006). Role of lipids and actin in the formation of clathrin-coated pits. Exp Cell Res *312*, 4036-4048.

Brodsky,F.M., Chen,C.Y., Knuehl,C., Towler,M.C., Wakeham,D.E. (2001). Biological basket weaving: formation and function of clathrin-coated vesicles. Annu Rev Cell Dev Biol *17*, 517-568.

Chvatchko,Y., Howald,I., Riezman,H. (1986). Two yeast mutants defective in endocytosis are defective in pheromone response. Cell *46*, 355-364.

Conner,S.D., Schmid,S.L. (2002). Identification of an adaptor-associated kinase, AAK1, as a regulator of clathrin-mediated endocytosis. J Cell Biol *156*, 921-929.

Cope,M.J., Yang,S., Shang,C., Drubin,D.G. (1999). Novel protein kinases Ark1p and Prk1p associate with and regulate the cortical actin cytoskeleton in budding yeast. J Cell Biol *144*, 1203-1218.

Cormack,R.S., Somssich,I.E. (1997). Rapid amplification of genomic ends (RAGE) as a simple method to clone flanking genomic DNA. Gene *194*, 273-276.

Dai,J., Sheetz,M.P. (1995). Regulation of endocytosis, exocytosis, and shape by membrane tension. Cold Spring Harb.Symp.Quant.Biol *60*, 567-571.

Davis,N.G., Horecka,J.L., Sprague,G.F., Jr. (1993). Cis- and trans-acting functions required for endocytosis of the yeast pheromone receptors. J Cell Biol *122*, 53-65.

D'Hondt,K., Heese-Peck,A., Riezman,H. (2000). Protein and lipid requirements for endocytosis. Annu Rev Genet. *34*, 255-295.

Dulic,V., Egerton,M., Elguindi,I., Raths,S., Singer,B., Riezman,H. (1991). Yeast endocytosis assays. Methods Enzymol. *194*, 697-710.

Engqvist-Goldstein,A.E., Drubin,D.G. (2003). Actin assembly and endocytosis: from yeast to mammals. Annu Rev Cell Dev Biol *19*, 287-332.

Fazi,B., Cope,M.J., Douangamath,A., Ferracuti,S., Schirwitz,K., Zucconi,A., Drubin,D.G., Wilmanns,M., Cesareni,G., Castagnoli,L. (2002). Unusual binding properties of the SH3 domain of the yeast actin-binding protein Abp1: structural and functional analysis. J Biol Chem *277*, 5290-5298.

Fujimoto,L.M., Roth,R., Heuser,J.E., Schmid,S.L. (2000). Actin assembly plays a variable, but not obligatory role in receptor-mediated endocytosis in mammalian cells. Traffic. *1*, 161-171.

Geli,M.I., Riezman,H. (1998). Endocytic internalization in yeast and animal cells: similar and different. J Cell Sci *111 (Pt 8)*, 1031-1037.

Gottlieb,T.A., Ivanov,I.E., Adesnik,M., Sabatini,D.D. (1993). Actin microfilaments play a critical role in endocytosis at the apical but not the basolateral surface of polarized epithelial cells. J Cell Biol *120*, 695-710.

Henry,K.R., D'Hondt,K., Chang,J.S., Nix,D.A., Cope,M.J., Chan,C.S., Drubin,D.G., Lemmon,S.K. (2003). The actin-regulating kinase Prk1p negatively regulates Scd5p, a suppressor of clathrin deficiency, in actin organization and endocytosis. Curr Biol *13*, 1564-1569.

Hicke,L. (2001). A new ticket for entry into budding vesicles-ubiquitin. Cell *106*, 527-530.

Higgins,M.K., McMahon,H.T. (2002). Snap-shots of clathrin-mediated endocytosis. Trends Biochem Sci *27*, 257-263.

Howard,J.P., Hutton,J.L., Olson,J.M., Payne,G.S. (2002). Sla1p serves as the targeting signal recognition factor for NPFX(1,2)D-mediated endocytosis. J Cell Biol *157*, 315-326.

Huang,B., Zeng,G., Ng,A.Y., Cai,M. (2003). Identification of novel recognition motifs and regulatory targets for the yeast actin-regulating kinase Prk1p. Mol Biol Cell *14*, 4871-4884.

Huxley et al., 1990 C. Huxley, E.D. Green and I. Dunham, Rapid assessment of *S. cerevisiae* mating type by PCR, *Trends Genet.* **6** (1990), p. 236.

Jackman,M.R., Shurety,W., Ellis,J.A., Luzio,J.P. (1994). Inhibition of apical but not basolateral endocytosis of ricin and folate in Caco-2 cells by cytochalasin D. J Cell Sci *107 (Pt 9)*, 2547-2556.

Jonsdottir,G.A., Li,R. (2004). Dynamics of yeast Myosin I: evidence for a possible role in scission of endocytic vesicles. Curr Biol *14*, 1604-1609.

Kaksonen,M., Sun,Y., Drubin,D.G. (2003). A pathway for association of receptors, adaptors, and actin during endocytic internalization. Cell *115*, 475-487.

Kaksonen,M., Toret,C.P., Drubin,D.G. (2005). A modular design for the clathrin- and actin-mediated endocytosis machinery. Cell *123*, 305-320.

Kaksonen,M., Toret,C.P., Drubin,D.G. (2006). Harnessing actin dynamics for clathrin-mediated endocytosis. Nat Rev Mol Cell Biol *7*, 404-414.

Kilmartin,J.V., Adams,A.E. (1984). Structural rearrangements of tubulin and actin during the cell cycle of the yeast Saccharomyces. J Cell Biol *98*, 922-933.

Kirchhausen,T. (2000). Clathrin. Annu Rev Biochem *69*, 699-727.

Kohtz,D.S., Hanson,V., Puszkin,S. (1990). Novel proteins mediate an interaction between clathrin-coated vesicles and polymerizing actin filaments. Eur.J Biochem *192*, 291-298.

Kron,S.J., Gow,N.A. (1995). Budding yeast morphogenesis: signalling, cytoskeleton and cell cycle. Curr Opin Cell Biol *7*, 845-855.

Lamaze,C., Fujimoto,L.M., Yin,H.L., Schmid,S.L. (1997). The actin cytoskeleton is required for receptor-mediated endocytosis in mammalian cells. J Biol Chem *272*, 20332-20335.

Lechler,T., Shevchenko,A., Li,R. (2000). Direct involvement of yeast type I myosins in Cdc42-dependent actin polymerization. J Cell Biol *148*, 363-373.

Lew,D.J., Reed,S.I. (1993). Morphogenesis in the yeast cell cycle: regulation by Cdc28 and cyclins. J Cell Biol *120*, 1305-1320.

Lew,D.J., Reed,S.I. (1995). A cell cycle checkpoint monitors cell morphogenesis in budding yeast. J Cell Biol *129*, 739-749.

Lippincott,J., Li,R. (1998). Sequential assembly of myosin II, an IQGAP-like protein, and filamentous actin to a ring structure involved in budding yeast cytokinesis. J Cell Biol *140*, 355-366.

Liu,J., Kaksonen,M., Drubin,D.G., Oster,G. (2006). Endocytic vesicle scission by lipid phase boundary forces. Proc Natl Acad Sci U S A *103*, 10277-10282.

Luo,W., Chang,A. (1997). Novel genes involved in endosomal traffic in yeast revealed by suppression of a targeting-defective plasma membrane ATPase mutant. J Cell Biol *138*, 731-746.

May,R.C., Machesky,L.M. (2001). Phagocytosis and the actin cytoskeleton. J Cell Sci *114*, 1061-1077.

McNiven,M.A., Cao,H., Pitts,K.R., Yoon,Y. (2000). The dynamin family of mechanoenzymes: pinching in new places. Trends Biochem Sci *25*, 115-120.

Merrifield,C.J. (2004). Seeing is believing: imaging actin dynamics at single sites of endocytosis. Trends Cell Biol *14*, 352-358.

Merrifield,C.J., Feldman,M.E., Wan,L., Almers,W. (2002). Imaging actin and dynamin recruitment during invagination of single clathrin-coated pits. Nat Cell Biol *4*, 691-698.

Merrifield,C.J., Perrais,D., Zenisek,D. (2005). Coupling between clathrin-coated-pit invagination, cortactin recruitment, and membrane scission observed in live cells. Cell *121*, 593-606.

Mulholland,J., Preuss,D., Moon,A., Wong,A., Drubin,D., Botstein,D. (1994). Ultrastructure of the yeast actin cytoskeleton and its association with the plasma membrane. J Cell Biol *125*, 381-391.

Munn,A.L. (2001). Molecular requirements for the internalisation step of endocytosis: insights from yeast. Biochim.Biophys.Acta *1535*, 236-257.

Munn,A.L., Riezman,H. (1994). Endocytosis is required for the growth of vacuolar H(+)-ATPase-defective yeast: identification of six new END genes. J Cell Biol *127*, 373-386.

Munn,A.L., Stevenson,B.J., Geli,M.I., Riezman,H. (1995). end5, end6, and end7: mutations that cause actin delocalization and block the internalization step of endocytosis in Saccharomyces cerevisiae. Mol Biol Cell *6*, 1721-1742.

Musacchio,A., Smith,C.J., Roseman,A.M., Harrison,S.C., Kirchhausen,T., Pearse,B.M. (1999). Functional organization of clathrin in coats: combining electron cryomicroscopy and X-ray crystallography. Mol Cell *3*, 761-770.

Newpher,T.M., Smith,R.P., Lemmon,V., Lemmon,S.K. (2005). In vivo dynamics of clathrin and its adaptor-dependent recruitment to the actin-based endocytic machinery in yeast. Dev Cell *9*, 87-98.

Nicholson-Dykstra,S., Higgs,H.N., Harris,E.S. (2005). Actin dynamics: growth from dendritic branches. Curr Biol *15*, R346-R357.

Novick,P., Botstein,D. (1985). Phenotypic analysis of temperature-sensitive yeast actin mutants. Cell *40*, 405-416.

Ohno,H., Stewart,J., Fournier,M.C., Bosshart,H., Rhee,I., Miyatake,S., Saito,T., Gallusser,A., Kirchhausen,T., Bonifacino,J.S. (1995). Interaction of tyrosine-based sorting signals with clathrin-associated proteins. Science *269*, 1872-1875.

Olusanya,O., Andrews,P.D., Swedlow,J.R., Smythe,E. (2001). Phosphorylation of threonine 156 of the mu2 subunit of the AP2 complex is essential for endocytosis in vitro and in vivo. Curr Biol *11*, 896-900.

Pearse,B.M. (1976). Clathrin: a unique protein associated with intracellular transfer of membrane by coated vesicles. Proc Natl Acad Sci U S A *73*, 1255-1259.

Pearse,B.M., Robinson,M.S. (1990). Clathrin, adaptors, and sorting. Annu Rev Cell Biol *6*, 151-171.

Pelkmans,L., Puntener,D., Helenius,A. (2002). Local actin polymerization and dynamin recruitment in SV40-induced internalization of caveolae. Science *296*, 535-539.

Peter,B.J., Kent,H.M., Mills,I.G., Vallis,Y., Butler,P.J., Evans,P.R., McMahon,H.T. (2004). BAR domains as sensors of membrane curvature: the amphiphysin BAR structure. Science *303*, 495-499.

Pollard,T.D. (1990). Actin. Curr Opin Cell Biol *2*, 33-40.

Pollard,T.D., Borisy,G.G. (2003). Cellular motility driven by assembly and disassembly of actin filaments. Cell *112*, 453-465.

Qualmann,B., Kessels,M.M. (2002). Endocytosis and the cytoskeleton. Int.Rev Cytol. *220*, 93-144.

Raths,S., Rohrer,J., Crausaz,F., Riezman,H. (1993). end3 and end4: two mutants defective in receptor-mediated and fluid-phase endocytosis in Saccharomyces cerevisiae. J Cell Biol *120*, 55-65.

Riezman,H. (1985). Endocytosis in yeast: several of the yeast secretory mutants are defective in endocytosis. Cell *40*, 1001-1009.

Rodal,A.A., Kozubowski,L., Goode,B.L., Drubin,D.G., Hartwig,J.H. (2005). Actin and septin ultrastructures at the budding yeast cell cortex. Mol Biol Cell *16*, 372-384.

Rodal,A.A., Manning,A.L., Goode,B.L., Drubin,D.G. (2003). Negative regulation of yeast WASp by two SH3 domain-containing proteins. Curr Biol *13*, 1000-1008.

Rose,M.D.W.F.a.H.P. (1990). Methods in Yeast Genetics: A Laboratory Course Manual. Cold Spring Harbor Laboratory Press, Cold Spring Harbor, New York.

ROTH,T.F., PORTER,K.R. (1964). YOLK PROTEIN UPTAKE IN THE OOCYTE OF THE MOSQUITO AEDES AEGYPTI. L. J Cell Biol *20*, 313-332.

Salisbury,J.L., Condeelis,J.S., Satir,P. (1980). Role of coated vesicles, microfilaments, and calmodulin in receptor-mediated endocytosis by cultured B lymphoblastoid cells. J Cell Biol *87*, 132-141.

Sambrook, J., Fritsch, E.F., and Maniatis, T., in Molecular Cloning: A Laboratory Manual. Cold Spring Harbor Laboratory Press, NY, Vol. 1, 2, 3 (1989).

Sanders,S.L., Field,C.M. (1994). Cell division. Septins in common? Curr Biol *4*, 907-910.

Santini,F., Gaidarov,I., Keen,J.H. (2002). G protein-coupled receptor/arrestin3 modulation of the endocytic machinery. J Cell Biol *156*, 665-676.

Schmid,S.L. (1992). The mechanism of receptor-mediated endocytosis: more questions than answers. Bioessays *14*, 589-596.

Shupliakov,O., Bloom,O., Gustafsson,J.S., Kjaerulff,O., Low,P., Tomilin,N., Pieribone,V.A., Greengard,P., Brodin,L. (2002). Impaired recycling of synaptic vesicles after acute perturbation of the presynaptic actin cytoskeleton. Proc Natl Acad Sci U S A *99*, 14476-14481.

Sirotkin,V., Beltzner,C.C., Marchand,J.B., Pollard,T.D. (2005). Interactions of WASp, myosin-I, and verprolin with Arp2/3 complex during actin patch assembly in fission yeast. J Cell Biol *170*, 637-648.

Smythe,E., Ayscough,K.R. (2003). The Ark1/Prk1 family of protein kinases. Regulators of endocytosis and the actin skeleton. EMBO Rep. *4*, 246-251.

Sun,Y., Martin,A.C., Drubin,D.G. (2006). Endocytic internalization in budding yeast requires coordinated actin nucleation and myosin motor activity. Dev Cell *11*, 33-46.

Tan,P.K., Howard,J.P., Payne,G.S. (1996). The sequence NPFXD defines a new class of endocytosis signal in Saccharomyces cerevisiae. J Cell Biol *135*, 1789-1800.

Toshima,J., Toshima,J.Y., Duncan,M.C., Cope,J.T., Sun,Y., Martin,A.C., Anderson,S., Yates,J.R., III, Mizuno,K., Drubin,D.G. (2006). Negative

Regulation of Yeast Eps15-like Arp2/3 Complex Activator, Pan1p, by the Hip1R-related Protein, Sla2p, during Endocytosis. Mol Biol Cell.

Umeda,A., Meyerholz,A., Ungewickell,E. (2000). Identification of the universal cofactor (auxilin 2) in clathrin coat dissociation. Eur.J Cell Biol *79*, 336-342.

Vida,T.A., Emr,S.D. (1995). A new vital stain for visualizing vacuolar membrane dynamics and endocytosis in yeast. J Cell Biol *128*, 779-792.

Watson,H.A., Cope,M.J., Groen,A.C., Drubin,D.G., Wendland,B. (2001). In vivo role for actin-regulating kinases in endocytosis and yeast epsin phosphorylation. Mol Biol Cell *12*, 3668-3679.

Welch,M.D., Holtzman,D.A., Drubin,D.G. (1994). The yeast actin cytoskeleton. Curr Opin Cell Biol *6*, 110-119.

Welch,M.D., Mullins,R.D. (2002). Cellular control of actin nucleation. Annu Rev Cell Dev Biol *18*, 247-288.

Wendland,B., McCaffery,J.M., Xiao,Q., Emr,S.D. (1996). A novel fluorescence-activated cell sorter-based screen for yeast endocytosis mutants identifies a yeast homologue of mammalian eps15. J Cell Biol *135*, 1485-1500.

Wilde,A., Brodsky,F.M. (1996). In vivo phosphorylation of adaptors regulates their interaction with clathrin. J Cell Biol *135*, 635-645.

Yarar,D., Waterman-Storer,C.M., Schmid,S.L. (2005). A dynamic actin cytoskeleton functions at multiple stages of clathrin-mediated endocytosis. Mol Biol Cell *16*, 964-975.

Young,M.E., Cooper,J.A., Bridgman,P.C. (2004). Yeast actin patches are networks of branched actin filaments. J Cell Biol *166*, 629-635.

Zeng,G., Cai,M. (1999). Regulation of the actin cytoskeleton organization in yeast by a novel serine/threonine kinase Prk1p. J Cell Biol *144*, 71-82.

Zeng,G., Yu,X., Cai,M. (2001). Regulation of yeast actin cytoskeleton-regulatory complex Pan1p/Sla1p/End3p by serine/threonine kinase Prk1p. Mol Biol Cell *12*, 3759-3772.

Publication

Mingji Jin and Mingjie Cai

A Novel Function of Arp2p in Mediating Prk1p-specific Regulation of Actin and Endocytosis in Yeast.

MBC in Press, published October 31, 2007 as 10.1091/mbc.E07-06-0530